Spring 2018

GIS-based spatial analysis coupled with geophysical imaging to identify and evaluate factors that control the formation of karst sinkholes in southwestern Missouri

Shishay T. Kidanu

Department: Geosciences and Geological and Petroleum Engineering

GIS-BASED SPATIAL ANALYSIS COUPLED WITH GEOPHYSICAL IMAGING TO IDENTIFY AND EVALUATE FACTORS THAT CONTROL THE FORMATION OF KARST SINKHOLES IN SOUTHWESTERN MISSOURI

By

SHISHAY TADIOS KIDANU

A DISSERTATION

Presented to the Faculty of the Graduate School of the

MISSOURI UNIVERSITY OF SCIENCE AND TECHNOLOGY

In Partial Fulfillment of the Requirements for the Degree

DOCTOR OF PHILOSOPHY

in

GEOLOGICAL ENGINEERING

2018

Approved by

Neil L. Anderson, Advisor
J. David Rogers
Kelly H. Liu
Evgeniy V. Torgashov
Lesley H. Sneed

PUBLICATION DISSERTATION OPTION

This dissertation is prepared in publication format and is consisting of the following three research papers:

Paper I, Pages 4-28, entitled "Using GIS-based Spatial Analysis to Determine Factors Influencing the Formation of Sinkholes in Greene County, Missouri. This paper is published in *Environmental & Engineering Geoscience*, Vol. XXIV, No. 2, February 2018, pp. 1–11

Paper II, Pages 29-51, entitled "ERT-based Investigation of a Sinkhole in Greene County, Missouri" This paper is published in *AIMS Geosciences Journal (May 2016)*. AIMS Geosciences, 2 (2): 99-115 DOI: 10.3934/geosci.2016.2.99

Paper III, Pages 52-70, entitled "3D-Electrical Resistivity Tomography imaging of the subsurface structure of a sinkhole in Greene County, Missouri". This manuscript is submitted to *AIMS Geosciences Journal* in March 2018.

ABSTRACT

Sinkholes are inherent features of the karst terrain underlying much of Greene County, Missouri. These features present hazards and engineering challenges to existing infrastructure unknowingly constructed on a seemingly benign ground surface. The primary objective of this research was to investigate the physical processes chiefly responsible for triggering the seemingly random distribution of sinkholes in the study area. This research employed an integrated approach encompassing regional scale GIS-based spatial analyses and site-specific geophysical data. GIS-based spatial analysis was employed to identify significant physical factors that appeared to influence the formation and distribution of sinkholes. Seven out of the twelve most cited factors influencing sinkhole development were identified in the study area. These factors were: overburden thickness, depth-to-groundwater, slope of the ground surface, distance to the nearest water course, distance to the nearest geologic structures, distance to nearest springs, and distance to the nearest roads.

In the site-specific geophysical investigations, two dimensional (2D) and pseudo three dimensional (3D) - ERT, MASW, and borehole data were used to characterize the subsurface morphology of the karstified soil-bedrock interface in five selected sinkholes. From the interpretation of the 2D and pseudo 3D-ERT profiles, it was determined that four of the five sinkholes occurred at the intersections of regional systematic joint sets. The joint sets are characterized by a linear, visually prominent zones of low resistivity. The relatively low resistivity values are attributed to vertical seepage and the associated piping of fine-grained soils through preexisting fractures (often widened by solutioning).

ACKNOWLEDGMENTS

I would like to express my most sincere appreciation and deep sense of gratitude to Dr. Neil Anderson, my advisor and chairman of the dissertation committee, for his great support to me throughout the course of this research. Without his financial support and his advice, encouragement, constructive criticisms and comments, this research would not have been successful. I also wish to express my profound gratitude to Dr. J. David Rogers for his financial support, guidance, stimulating suggestions and reviewing manuscripts during the research period. I would like to thank Dr. Evgeniy Torgashov for his support and valuable discussions on my research work. I also wish to acknowledge the contributions and advice of the other members of the dissertation committee, namely, Dr. Kelly Liu, Dr. Maochen Ge and Dr. Lesley Sneed.

I would like to thank the faculty and staff of the Department of Geosciences and Geological and Petroleum Engineering and to my colleagues who in one way or another contributed in this research. I would also like to express my special gratitude to my family and friends for their outstanding love, encouragement and support during my study.

Last but not least, all my gratitude to my amazing, lovely and caring wife, Aden Legese and my lovely kids Nahom and Saron. Thank you for your love, support and understanding.

TABLE OF CONTENTS

Page

LIST OF ILLUSTRATIONS

PAPER I Page

PAPER II

PAPER III

LIST OF TABLES

PAPER I Page

PAPER II

1. INTRODUCTION

Karst area is formed in carbonate and evaporitic rocks, primarily by dissolution and is characterized by numerous sinkholes, losing streams, springs, caves, and other related features. Karst area is one of the most challenging environment when dealing with groundwater, engineering and environmental issues (Chalikakis, 2011). Sinkholes are one of the most common karst structures in the world (Festa et al, 2012) and are also one of the most important hazard in karst areas (e.g. Waltham et al., 2005; Gutiérrez, 2010). Catastrophically collapsing sinkholes may lead to fatal accidents with losses in human life and ground deformation associated with the development of subsidence sinkholes may cause severe damage to infrastructures (Carbonel et al. 2014). Furthermore, sinkholes are frequently associated with hazardous processes such as; differential compaction of sinkhole deposits, typically underlain by irregular rockhead; flooding of depressions by runoff concentration, water table rise, or back flooding (e.g. Zhou, 2007); water leakage at dams and other hydraulic structures (e.g. Milanovic, 2000), or groundwater pollution.

According to the U.S.Karst map published by AGI (Veni et. al.2001), most of the southern part of Missouri, is underlined by carbonate rock and recognized as a karst terrain. The study area, Greene County, Missouri, is part of the Ozarks physiographic region and is underlain mainly by Mississippian Age limestone which is highly susceptible to karst processes. Thousands of sinkholes have been identified in the state of Missouri and Greene County is one of the counties in the state known for the presence of sinkholes (Ismail and Anderson, 2012).

Sinkhole formation processes involve a combination of geologic, geomorphologic, hydrologic, and anthropogenic influencing factors that interact in the subsurface

(Kaufmann, 2008; Galve, 2009; Doctor, 2012). Determining the main controlling factors and understanding the nature of interaction among the factors helps to determine where and how an individual sinkhole may form. The interactions among the influencing factors are mainly in the subsurface and are usually hidden from the scope of direct observation and hence, it is unlikely to predict the formation of an individual sinkhole at a given place. Nevertheless, analysis of spatial statistical relationships between sinkhole density and the associated possible influencing factors can help to determine the main factors controlling the formation and spatial distribution of sinkholes. Knowing the major controlling factors and the relationship among them helps to provide an objective means of parameter weighting in models of sinkhole susceptibility or hazard mapping which in turn helps for land use planning and landscape management to mitigate the risks of future sinkhole occurrences. A clustering pattern analysis on the spatial distribution of the sinkholes in the area has been done to see if the distribution is clustered or not. The cluster analysis was done using the Nearest Neighbor Analysis (NNA) tool in ArcGIS 10.2. The NNA result indicated that the sinkholes are significantly clustered with a p-value ($p = 0.000000$), and Nearest Neighbor Ratio (observed mean distance/expected mean distance) of 0.52.

The significant clustering implies that it is very unlikely some random process created the observed distribution. Rather, the clustering indicates that there is an underlying process with a key set of influencing factors responsible for the formation and distribution of the sinkholes in the area. The NNA analysis result supported the assumption that the sinkhole formation and distribution is not formed due to a random process rather it is the result of a certain process controlled by a set of influencing factors. Determining the main factors controlling the formation and spatial distribution of sinkholes is important input for

prediction of future sinkhole occurrence in the area and this helps for better land use management practices, including conservation of natural resources, ground-water management, and environmental protection.

The second major concern is the impacts of the existing active sinkholes and sinkhole developments. Investigating the development mechanism and subsurface structure of existing sinkholes and characterizing the nature and 3D configuration of the geology beneath them enables us to predict their long-term impact and chance of reactivation and provide applicable corrective measures. Some of the facts that necessitate such kind of investigation on existing sinkholes are: (i) from an engineering standpoint it is important to locate and characterize soil piping zone, filled voids, and buried bedrock fractures, ravel zone as they may reactivate in the course of time; (ii) for hydrogeological studies it may be desirable to determine whether a sinkhole functions as a groundwater flow conduit connecting surface and subsurface water. Therefore, site-specific sinkhole investigation is required to understand the subsurface structure and development mechanism of existing sinkholes to provide proper mitigation measure to avoid or minimize their impacts. Effective sinkhole investigation should integrate a variety of investigative approaches that include geological, geophysical, and geomorphological analysis (Gutiérrez, 2008).

PAPER

I. USING GIS-BASED SPATIAL ANALYSIS TO DETERMINE FACTORS INFLUENCING FORMATION OF SINKHOLES IN GREENE COUNTY, MISSOURI

SHISHAY T. KIDANU[1*], email: stkq7f@mst.edu

NEIL L. ANDERSON[1], email: nanders@mst.edu

J. DAVID ROGERS[1], email: rogersda@mst.edu

[1]Department of Geosciences and Geological and Petroleum Engineering, Missouri University of Science and Technology, Rolla, MO 65409, USA

[*]Corresponding author email: stkq7f@mst.edu

ABSTRACT

Sinkholes are inherent features of the karst terrain of Greene County, Missouri, which present hazards and engineering challenges to construction / infrastructure development. Analysis of relationships between the spatial distribution of sinkholes and possible influencing factors can help in understanding the controls involved in the formation of sinkholes. The spatial analysis outlined herein can aid in the assessment of potential sinkhole hazards. In this research, GIS-Based Ordinary Least Squares Regression (OLS) and Geographically Weighted Regression (GWR) methods were used to determine and evaluate principal factors appearing to influence the formation and distribution of karst sinkholes. From the OLS result, seven out of twelve possible influencing factors were found to exert significant control on sinkhole formation processes in the study area. These factors are overburden thickness, depth-to-groundwater, slope of the ground surface,

distance to the nearest surface drainage line, distance to nearest geological structure (such as faults or folds), distance to the nearest road, and distance to the nearest spring. These factors were then used as independent variables in the GWR model. The GWR model examined the spatial non-stationarity among the various factors, and demonstrated better performance over OLS. GWR model coefficient estimates for each variable were mapped. These maps provide spatial insights into the influence of the variables on sinkhole densities throughout the study area. GWR spatial analysis appears to be an effective approach to understand sinkhole influencing factors. The results could be useful to provide an objective means of parameter weighting in models of sinkhole susceptibility or hazard mapping.

Keywords: Geographic Information Systems (GIS), Sinkhole, Geographic Weighted Regression (GWR), Ordinary Least Squares Regression (OLS), Greene County.

1. INTRODUCTION

Karst topography develops on carbonate and evaporitic rocks, primarily by dissolution of soluble minerals. It is usually characterized by numerous sinkholes, caves, losing streams, springs, and preferential seepage pathways often influenced by geologic structure, stratigraphy, and watershed area. Karst is often a challenging environment when dealing with groundwater, engineering, and environmental issues (Chalikakis, 2011). Sinkholes are one of the most significant hazards in karst areas (Waltham et al., 2005; Gutiérrez, 2010). Sinkholes that suddenly collapse can result in loss of human life and property; and ground deformation associated with subsidence often damage infrastructure, such as highways and utilities (Carbonel et al., 2014). Thousands of sinkholes have been

identified in the state of Missouri; Greene County, in particular, is one of the counties in the state most known for the occurrence of sinkholes.

The formation of sinkholes is influenced by a combination of interacting geologic, geomorphologic, hydrologic, and anthropogenic factors (Kaufmann, 2008; Galve, 2009; Doctor, 2012). Ascertaining the main influencing factors and understanding the nature of their interactions can enable researchers to better understand where and how individual sinkholes may appear. The interactions between influencing factors are frequently not obvious and are often hidden from direct observation, making it unlikely to predict the occurrence of an individual sinkhole at a specific site. Nevertheless, the analysis of the spatial statistical relationships between sinkhole density and the potential influencing factors could help determine the principal causal factors influencing the formation and general spatial distribution and density of sinkholes in a particular area. Identifying the major influencing factors and the interactive relationships between them should provide an objective means of parameter weighting that would be useful in any GIS-driven model examining sinkhole susceptibility for hazard mapping.

Geographic Information System (GIS) techniques have been employed in various types of geohazard zonation analyses for land use planning and landscape management (Rogers, 1997). GIS spatial data processing and analysis techniques can be used to facilitate handling and processing of large data sets for sinkhole susceptibility modeling and to determine and evaluate the factors influencing the formation of sinkholes. Researchers have used different spatial analytical approaches to model sinkhole susceptibility. The most commonly used approaches are those that use proximity of neighboring sinkholes (i.e., Drake and Ford, 1972; Magdalene and Alexander, 1995) or sinkhole density (i.e., Brook

and Allison, 1986; Orndorff et al., 2000). These approaches have sought to make a qualitative evaluation of the relation between sinkhole occurrence and the primary influencing factors (geologic, geomorphologic, hydrologic or anthropologic effects). Another approach is a heuristic model, in which weights are assigned to the factors that influence sinkhole susceptibility for risk assessment (i.e., Kaufmann, 2008). The main limitation of the heuristic approach is the subjectivity related to expert evaluation and the difficulty of reproducing the method for different geologic areas. Galve et al. (2009b) found that nearest neighbor and sinkhole density methods performed better than other techniques when identifying areas of sinkhole susceptibility, but those methods do not include sinkhole formation explanatory variables. Their ability to measure the influence of various factors on sinkhole development was limited (Doctor, 2012). The methods based on density and proximity may not satisfactorily identify sinkhole alignments; for instance, a sinkhole-prone belt determined by a fracture or a lithologic boundary may be missed in such susceptibility maps. The other classes of susceptibility modeling are probabilistic or statistical methodologies that derive the susceptibility models from the analysis of spatial statistical relationships between known sinkholes and a group of influencing factors (Galve, 2009).

Geographically Weighted Regression (GWR) is a relatively recent and sophisticated method of spatial statistical analysis that seeks to measure spatially varying relationships, such as the influence of controlling factors on sinkhole formation. GWR is a local regression version of the global Ordinary Least Squares regression (OLS) method. Geographically Weighted Regression (GWR) can be an effective tool to study spatial data relationships with spatial non-stationarity (Fotheringham et al., 2002). In this research,

GIS-Based global (Ordinary Least Squares, OLS) and spatial (Geographically Weighted Regression, GWR) multivariate regression methods were applied to evaluate and assess the variables controlling the formation of sinkholes in Greene County. The results suggest that there are seven variables that appear to be the principal sinkhole influencing factors. Moreover, coefficient surface maps for each influencing factor were generated to observe how each relationship between sinkhole occurrence and the influencing factors varied across the study area.

2. LOCATION AND GEOLOGY OF THE STUDY AREA

Greene County is located in southwestern Missouri (Figure 1) and is underlain mainly by Mississippian age Burlington-Keokuk Limestone (Figure 2). This bedrock underlies more than 70% of the county. About 98% of the sinkholes in Greene County are formed on Burlington-Keokuk Limestone bedrock. The study area encompasses about 1336 sq.km.

The Burlington-Keokuk Limestone is characterized by layers of limestone interbedded with thin layers of chert and the presence of chert nodules within the limestone layers. The limestone is a light gray, coarsely crystalline, and nearly pure calcite. Uneven dissolution of the Burlington-Keokuk Limestone has resulted in highly irregular bedrock-overburden interface (Fellows, 1970) and is characterized by the formation of prominent knobs (pinnacles) of bedrock bounded by deep troughs (grikes or “cutters”) caused by dissolution along fractures.

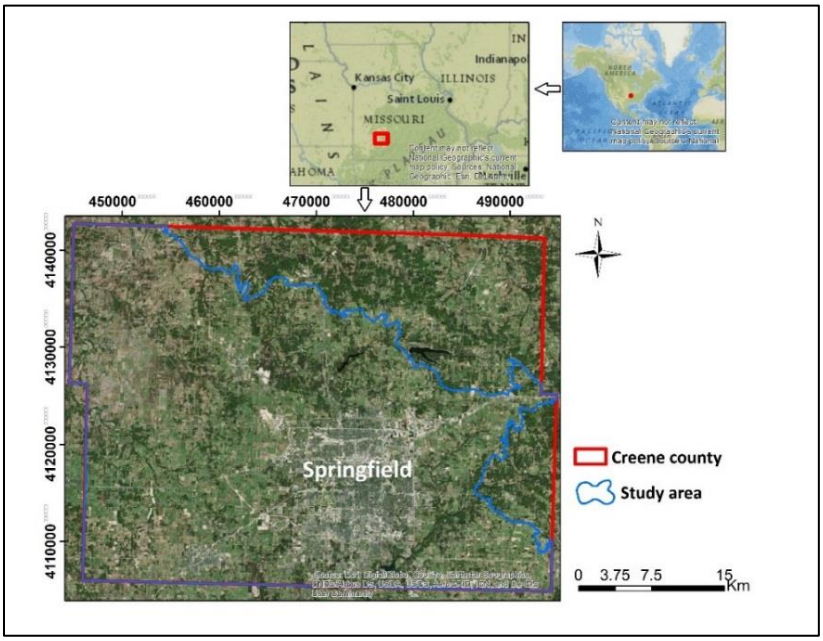

Figure 1. Location map of the study area.

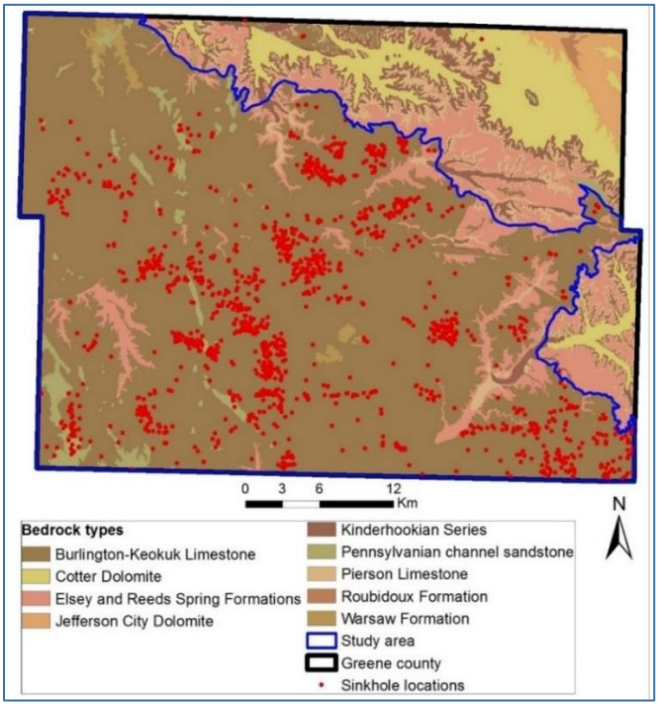

Figure 2. Geological and sinkhole locations map of Greene County. (ESRI data source: Missouri Geological Survey-GeoSTRAT).

3. DATASETS AND METHODOLOGY

3.1. DATASETS

A set of relevant ESRI (Environmental Systems Research Institute) datasets and digital maps of the study area were gathered from a variety of open sources e.g., Missouri Geological Survey-GeoSTRAT program (2016), Missouri Spatial Data Information Service (MSDIS, 2016), and United States Department of Agriculture (USDA, 2016). Further refinements, processing, and conversions were then made on the gathered datasets using ArcGIS 10.2® to derive a set of variables. The derived variables that were implemented in the multivariate regression modeling are sinkhole density (dependent variable) and a set of potential sinkhole influencing factors (independent variables). The independent variables consist of geological, geomorphic, hydrogeologic, and anthropogenic raster datasets. The ESRI datasets and digital maps, together with the corresponding derived variables are summarized in Table 1.

3.2. DEPENDENT AND INDEPENDENT VARIABLES

The sinkhole dataset of the study area was extracted from the publicly available Missouri sinkhole database of the Missouri Geological Survey in June 2016, and it shows the point locations of 1419 sinkholes (Figure 3). The Nearest Neighbor Analysis (NNA) tool in ArcGIS 10.2 was used to analyze the spatial distribution pattern of known sinkholes to ascertain if the distribution is random or not. NNA provides p-value and nearest neighbor ratio as indicators of predictive patterns. The p-value is the probability that some random process created the observed spatial pattern. If the Nearest Neighbor Analysis on the sinkhole distribution shows a clustered pattern, it is very unlikely that the observed pattern

is the result of random processes. Rather, it implies that there is an underlying process with a set of controlling factors responsible for the formation and distribution of the sinkholes in the study area.

The dependent variable used in the OLS and GWR analysis consisted of sinkhole density values of each sinkhole location, extracted from sinkhole density map. The sinkhole density map was generated using the kernel density tool in ArcGIS 10.2. A buffer size of 2500m was ascribed around each sinkhole location and used to calculate the kernel density. This size (2500m) was determined by using Multi-Distance Spatial Cluster Analysis (Ripleys K-function) tool in ArcGIS, which is useful in assessing possible scale effects that may be influencing spatially clustered sinkhole arrays.

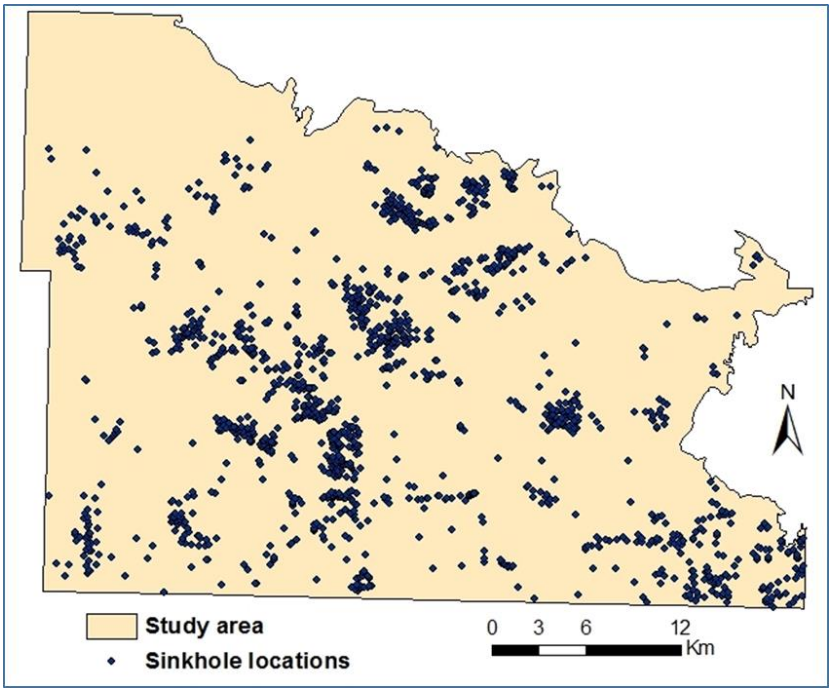

Figure 3. Sinkhole distribution map of the study area.

Table 1. Shows the gathered ESRI datasets and digital maps, data sources and the derived variables.

Main dataset/map	**Data sources**	**Derived variables**	**Cell size (mxm)**
Sinkhole locations (ESRI data)	Missouri Geological Survey-GeoSTRAT	Sinkhole density raster	50x50
Bedrock type (ESRI data)	Missouri Geological Survey-GeoSTRAT	Bedrock type map	--
Geologic structures (ESRI data)	Missouri Geological Survey-GeoSTRAT	Distance to nearest geological structure raster	50x50
Overburden thickness contour lines (ESRI data)	Missouri Spatial Data Information Service (MSDIS)	Overburden thickness raster	50x50
Depth to Groundwater contour lines (ESRI data)	Missouri Geological Survey-GeoSTRAT	Depth to Groundwater raster	50x50
Ground elevation contour lines (ESRI data)	Missouri Spatial Data Information Service (MSDIS)	DEM (Digital Elevation Model)	50x50
		Ground surface Slope	50x50
		Curvature (planar and profile)	50x50
Soil type map	United States Department of Agriculture	Soil type map	--
Drainage lines map	United States Department of Agriculture	Distance to nearest drainage line raster	50x50
Spring locations (ESRI data)	Missouri Geological Survey-GeoSTRAT	Distance to nearest spring raster	50x50
Missouri Highway/road feature data	http://www.mapcruzin.com/	Distance to nearest road raster	50x50

The independent variables are the raster data layers encompassing the potential sinkhole influencing factors. Twelve independent variables were considered for input into the model. These variables are: overburden thickness, depth-to-groundwater, distance to the nearest geological structure (faults, folds and other related tectonic structures), distance to the nearest drainage line, distance to the nearest spring, groundwater elevation, ground surface elevation (altitude), bedrock elevation, slope of the existing ground surface, distance to the nearest road, and ground surface curvature (planar and profile). Some potential influencing factors that include soil type, rate of groundwater drawdown, geochemical, and climatic processes could not be included in the sinkhole formation model due to paucity of data, insufficient data form, and model criteria.

3.3. MULTIVARIATE REGRESSION METHODS

Multivariate spatial regression analysis is a statistical technique that can examine, model, and explore spatial relationships among given variables across any designated area. In this research, it was used to evaluate possible relationships between sinkhole density and the physical factors believed to be influencing the sinkhole formation processes at the current time. When dealing with spatial data relationships, regression methods may assume that these relationships are consistent geographically (stationarity), or take into account the spatial locations of features, permitting the estimated parameters to vary locally (non-stationarity). The later assumption better reflects spatially varying relationships between dependent and independent (explanatory) variables, and usually results in improved model performance.

Ordinary Least Squares regression (OLS) is the most commonly employed regression technique and is usually the starting point for all spatial regression analysis

(ESRI, 2014). OLS provides a global model of the variable or process that one needs to understand or predict by creating a single regression equation to represent that process (ESRI, 2014). The OLS regression model with k, number of independent variables is of the form (Charlton and Fotheringham, 2009),

$$y = \beta_0 + \beta_1 x_1 + \beta_2 x_{2+} \beta_3 x_3 + \ldots + \beta_k x_k + \varepsilon$$

where y is the dependent variable and x_1 is the explanatory/independent variable. β_0 is the intercept of the line on the y-axis, and β_1 represents the slope coefficient for independent variable x_1. ε is a mean zero random error term with constant (but unknown) variance, and is normally distributed.

The ordinary least squares regression (OLS) method assumes that the spatial relationships between dependent and independent variables are static, and would not be efficient if there exists spatial non-stationarity in the relationships between the variables. When the relationship between variables under study exhibit non-stationarity (spatially varying) behavior, Geographically Weighted Regression (GWR), a local regression technique, is normally preferred.

Geographically Weighted Regression (GWR) is one of the most sophisticated applied methodologies for local regression analysis (Kalogirou and Hatzichristos, 2007; Brunsdon et al., 1996; Brunsdon et al., 1998). GWR allows for local (spatial) variables to be estimated (Fotheringham and Brunsdon, 1999). It allows examination of spatial non-stationarity of the factors influencing the formation and distribution of sinkholes. The GWR version of the OLS regression model extends the traditional regression framework by allowing parameters to be estimated locally (Charlton and Fotheringham, 2009), and can be expressed as:

$$Y_i = \beta_{0(ui,vi)} + \sum_{k=1}^{d} \beta_{k(ui,vi)} X_{ik} + \varepsilon_i \qquad i = 1, 2, \ldots, n$$

where Y_i is the dependent variable in spatial location with the coordinate (u_i, v_i); X_1, X_2, …,X_d are explanatory (independent) variables; and X_{ik} means the k-th explanatory variable in spatial location with coordinate (u_i, v_i); $\beta_0(u_i, v_i)$ represents the intercept value; β_k(ui, vi) is a set of values of coefficients at spatial location i.

Several researchers have used GWR to model spatially varying relationships or processes. Some examples include (i) the exploration of the relations between riverbank erosion and geomorphological controls (Atkinson et al., 2003); (ii) analysis of the relationship between geologic and hydrologic features and sinkhole occurrence (Doctor et al., 2012); (iii) the spatial simulation of regional land use patterns (Liao et al., 2010); (iv) assessing risk factors for malaria hotspots (Ndiath et al., 2015); (v) assessment of land subsidence potential (Blachowski, 2016); (vi) landslide susceptibility mapping (Arzu et al., 2010); and (vii) the exploration of spatial non-stationarity of fisheries survey data (Windle et al., 2010). In this research OLS followed by GWR were employed to analyze the influencing factors for the formation and distribution of sinkholes across the study area. A flow chart outlining the procedures and methods used in this study are summarized in Figure 4.

4. RESULTS AND DISCUSSIONS

4.1. SINKHOLE DENSITY AND CLUSTER ANALYSIS

Several authors (e.g., Brezinski, 2004; Zhou, 2003) have mentioned that in areas where active sinkholes have developed, there is a greater chance that new sinkholes will

form. Therefore, sinkhole density is an important factor in determining the areas most prone to sinkhole development. Kemmerly (1982) has asserted that cluster analysis may be applied to evaluate if the generation of new sinkholes is influenced by the location of the pre-existing sinkhole population.

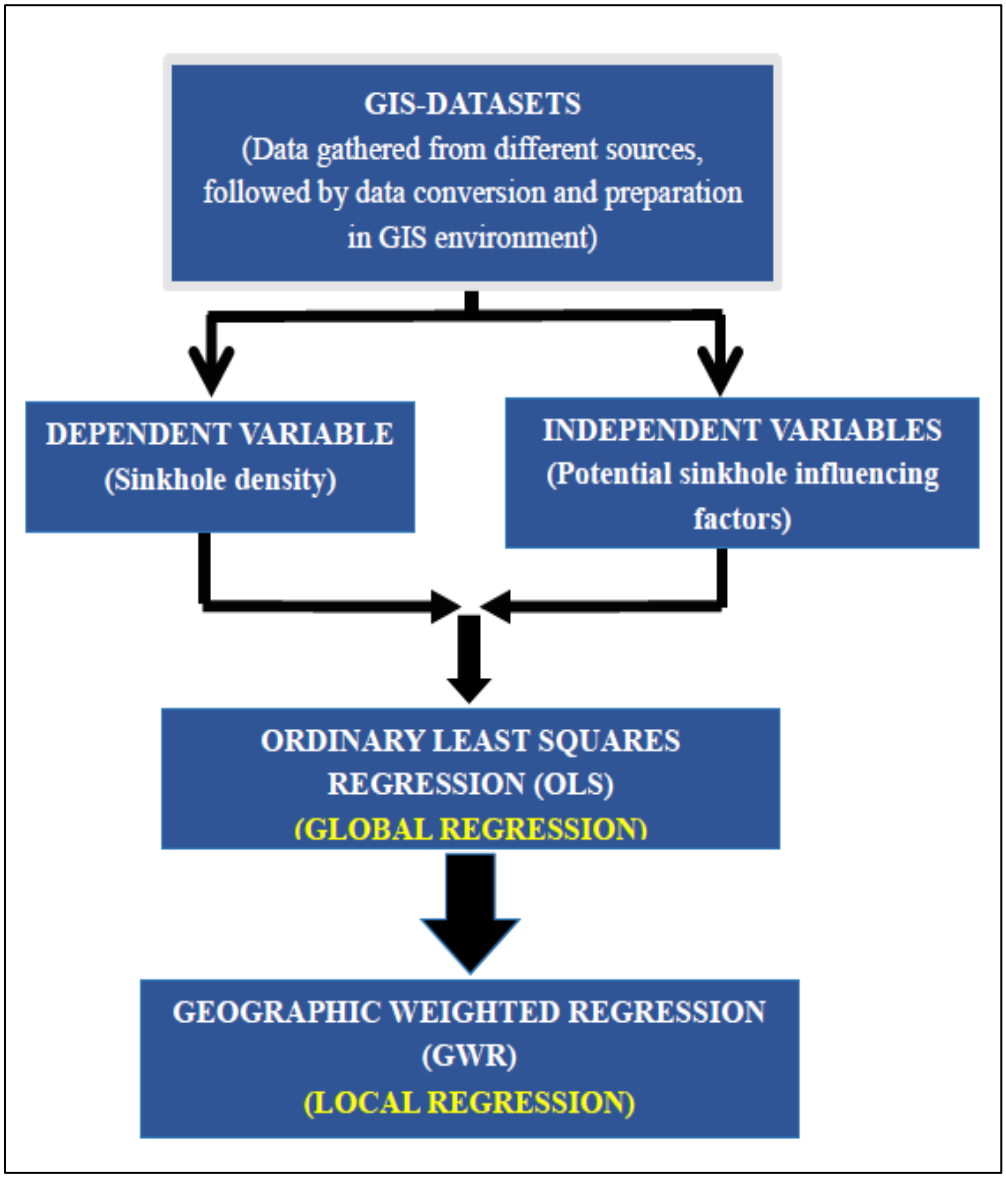

Figure 4. Flowchart showing the procedures and methods used in the study

Other authors (Hyatt et al., 1999; Gutiérrez-Santolalla et al., 2005b) have studied sinkhole distributions centered on manipulation of statistical values for prediction of future sinkholes. In this research, a sinkhole density dataset (Figure 5) was generated using the kernel density tool in ArcGIS along with cluster analysis using the Nearest Neighbor Analysis (NNA) tool to see if any spatial patterns of sinkholes were discernable. The NNA result (Figure 6) suggests that the sinkholes are significantly clustered, with a p-value (p = 0.000000), and nearest neighbor ratio (observed mean distance/expected mean distance) of 0.52. The significant clustering implies that it is very unlikely some random process created the observed distributions. Rather, the clustering indicates that there is an underlying process with a set of key influencing factors that is likely responsible for the formation and distribution of the sinkholes in the study area.

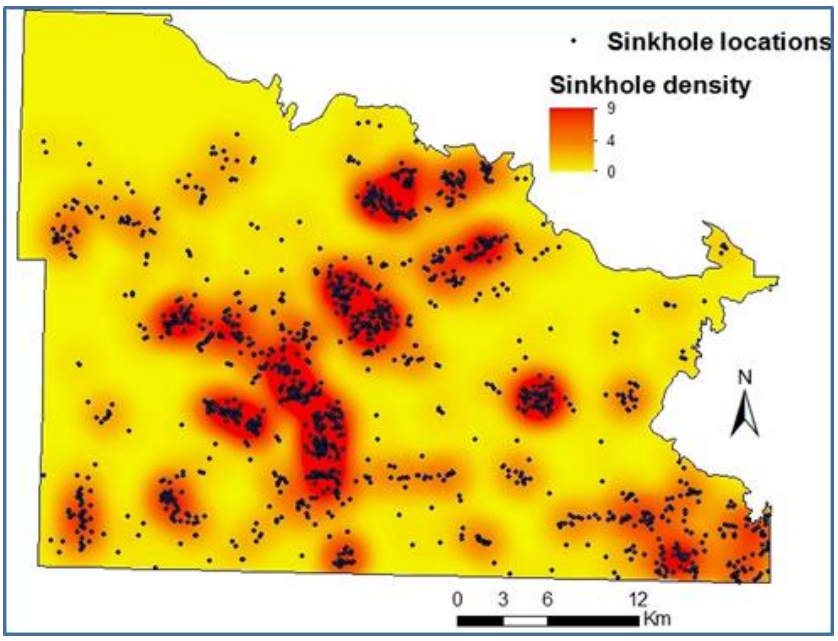

Figure 5. Map showing sinkhole locations (dots) and densities (number of sinkholes per sq.km).

After ascertaining the clustered nature of sinkhole distribution, the next logical question was “what” are the main factors controlling this observed clustered pattern? OLS followed by GWR analysis was employed to explore the spatial relationship between sinkhole density and the explanatory variables, so we could extract the significant controlling variables.

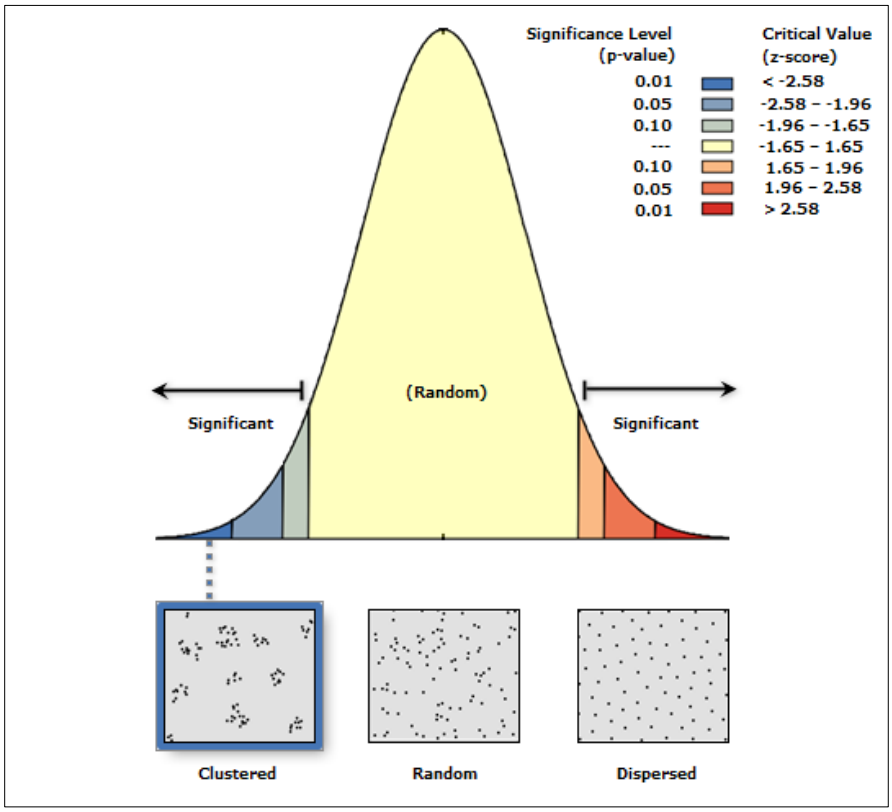

Nearest Neighbor Ratio:	0.522323	
z-score:	-34.423642	
p-value:	0.000000	

Figure 6. Results of Nearest Neighbor Analyses showing the sinkhole distribution pattern.

4.2. ORDINARY LEAST SQUARES REGRESSION (OLS) MODEL RESULTS

As mentioned previously, twelve potential sinkhole influencing factors were considered in the OLS analysis. A series of model checks were performed to evaluate the reliability of the OLS regression model. According to the Robust probability significant test results, ground surface curvature (both planar and profile), elevation to top of rock, and groundwater elevation were not significantly correlated with the dependent variable (sinkhole density), and were, therefore, removed from the model.

Another test was multicollinearity test, in which the Variance Inflation Factor (VIF) was employed to make sure that none of the explanatory variables were redundant. The rule of thumb for interpreting VIF values was that they should be less than 7.5, with smaller values representing better correlations. Variables with VIF values greater than 7.5 are generally removed from the model. The test results showed that the VIF values of all the variables were less than 7.5, except for ground surface elevation (altitude), elevation to top of rock, and groundwater elevation, so the ground surface elevation (altitude) variable was also removed from the model. After peforming all these model tests, seven of the twelve variables were selected as significant explanatory variables likely influencing the formation of sinkholes in the study area. These variables are; overburden thickness, distance to the nearest drainage line, depth to groundwater, slope of ground surface, distance to the nearest geological structure, distance to the nearest road, and distance to the nearest spring (Table 2) and their thematic maps are presented in Figure 7. The explanatory variables were selected on the basis of exhibiting robust probability statistics with low VIF values, in the range of 1.08 to 4.0 (Table 2). They also exhibit theoretically justifiable coefficient signs on a global scale. Overburden thickness, distance to nearest road, slope

of ground surface, and distance to nearest geological structure exhibit negative correlations with the occurrence of sinkholes, which suggests that, for example, areas closer to geological structures have a higher incidence of sinkhole occurrence than areas further away. The remaining factors, depth to groundwater, distance to nearest spring, and distance to nearest drainage line exhibit positive coefficient signs.

The result from the OLS model showed that the adjusted R^2 value is 0.570 and that the Akaike Information Criterion (AIC) value is 4853. This suggests that the OLS global model can explain about 57 % (adjusted R^2 = 0.570) of the variation in sinkhole density, with AIC = 4853. The adjusted R^2 and the AICc are statistics derived from the regression equation to quantify model performance (ESRI, 2014). The ANOVA returned a statistically significant F- statistic value = 157.84 and the Wald statistic has a significant Chi-squared value = 2443.37. These results indicate that the model formulation was statistically significant. The Jarque–Bera statistic returned a non-significant Chi-squared value = 3.42, indicating that the model's prediction is free from bias (i.e. the residuals have a normal distribution). All of these diagnostic tests suggests a fairly strong model, although one statistic, the Koenker test, was found to be statistically significant, which indicates the relationship between some or perhaps all of the explanatory variables and the dependent variable are non-stationary (spatially varying) across the study area. The reason for this is that some explanatory variables may be important for predicting the formation of the sinkhole in some locations, but not in other areas. The spatial autocorrelation test run on the OLS model's residuals with the Moran's I tool exhibited a clustered pattern. The presence of spatially clustered residuals, as well as the statistically significant value of the Koenker statistic in the OLS model, suggests the presence of spatial non-stationarity in the

data. This supports the premise that a local regression method can better explain the process than a global regression model (OLS). For these reasons, GWR was applied and it is evident that the model's fitness will likely be improved by incorporating GWR, which takes into account the spatial variability of factors.

Table 2. Summary statistics for OLS (Significant at ** 0.01 % level; * 5 % level).

Variables	**Coefficient values**	**Robust_Pr [b]**	**VIF**
Overburden thickness	-0.044726	0.00**	2.192135
Distance to nearest drainage line	0.002405	0.00**	1.321380
Depth to groundwater	0.023164	0.00**	4.004964
Distance to nearest road	-0.000845	0.00**	1.086326
Slope of ground surface	-0.153766	0.00**	1.270746
Distance to nearest geological structure	-0.000041	0.040*	1.156041
Distance to nearest spring	0.000207	0.00**	2.301522

4.3. GEOGRAPHICALLY WEIGHTED REGRESSION (GWR) MODEL RESULTS

As mentioned earlier, OLS appears to be the best starting point in building GWR models, so the GWR model was run using the same dependent variable and seven independent variables selected from the OLS analysis (Table 2).

The results of the GWR analysis showed that 86% (adjusted $R^2 = 0.8557$) of the variance in sinkhole density can be explained by the model, which is much higher than that

of OLS (57%). The AICc value for the GWR model was 758, whereas that derived from the OLS was 4853. Greater adjusted R^2, and smaller AICc values indicate that the GWR model (local regression) is superior to the OLS model (global regression), and has captured the spatial non-stationarity of variables.

GWR calculates different regression parameter values (e.g. coefficient) for each cell that can be mapped, so the spatial variations of parameters can be examined and observed visually. Coefficient surface maps for each explanatory variable were generated to ascertain how the relationship between sinkhole occurrence and the influencing factors varies across the study area. For example, coefficient maps of two variables (slope and depth to groundwater) are shown in Figure 8. These maps help us understand which of the influencing factors were most important in the sinkhole formation process and how the relations vary spatially. For instance, results derived from the global OLS model indicated that the slope variable has a negative relationship with sinkhole occurrence across the study area; however, according to the GWR analysis, the contribution of this variable to sinkhole occurrence spatially varies across the study area, with coefficients ranging from -0.44 to 0.23. The range of coefficient values suggest that the nature (positive or negative) and strength of the relationship varies spatially across the study area (Figure 8). Similarly, the coefficients of the other variables also vary across the study area, including: depth to groundwater (-0.02 to 0.06), overburden thickness (-1.66 to 0.11), distance to nearest spring (-0.00040 to 0.0014), distance to nearest geological structures (-0.00026 to 0.00050), distance to nearest drainage line (0.0000027 to 0.0033), and distance to neares road (-0.0018 to 0.0012).

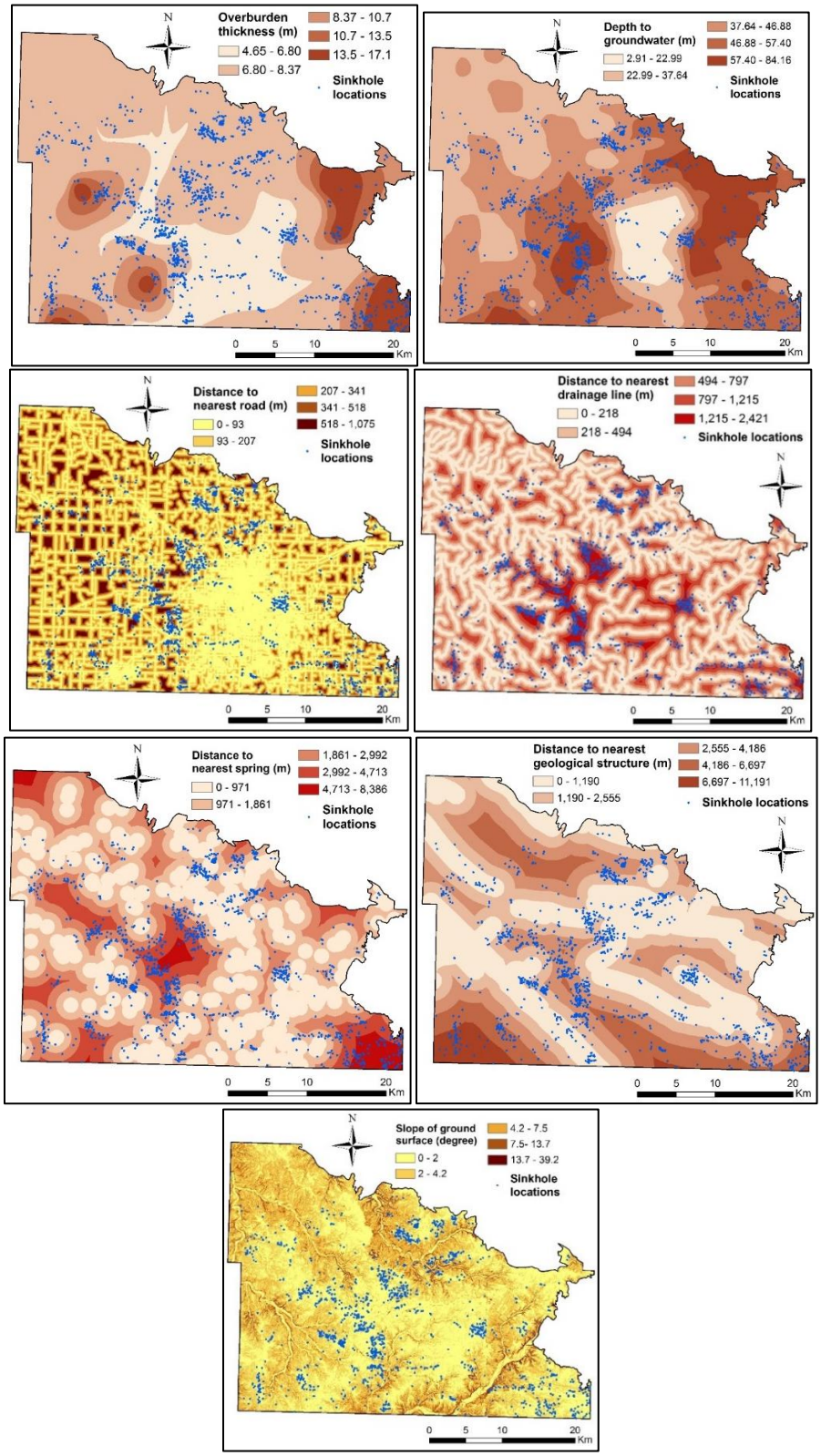

Figure 7. Thematic maps of seven independent variables in our regression (OLS and GWR) model.

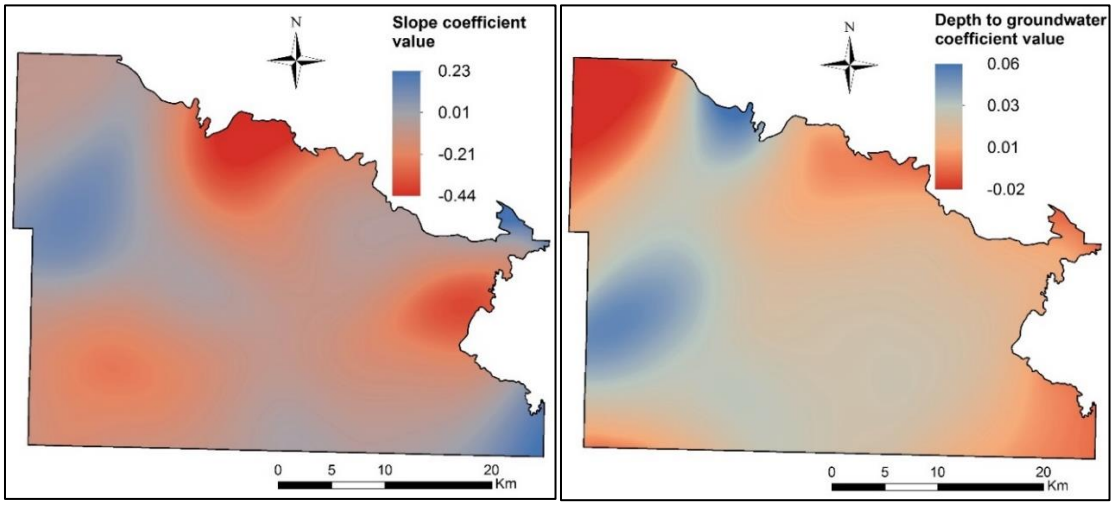

Figure 8. Slope and depth to groundwater coefficient surface maps derived from the GWR analysis.

5. CONCLUSIONS AND RECOMMENDATIONS

The Burlington-Keokuk Limestone bedrock underlies more than 70% of Greene County and 98 % of the identified sinkholes in the county (Missouri Geological Survey-GeoSTRAT, 2016) formed in this unit. Analysis of the sinkholes' spatial distribution and patterns suggest that the sinkholes are not randomly distributed, but are spatially clustered. This implies that there is a process controlled by a finite set of factors that promote the formation and development of karst sinkholes.

In this study GIS-based multivariate regression methods (OLS and GWR) were applied to evaluate the spatial relationships between potential sinkhole influencing factors (explanatory variables) and sinkhole density (dependent variable), with the aim of evaluating the significant controlling factors. The OLS analysis revealed that seven of the

twelve possible influencing factors considered in the analysis likely play important roles in triggering the formation of sinkholes. These factors are overburden thickness, slope of ground surface, depth to groundwater, distance to the nearest drainage line, distance to the nearest road, distance to the nearest geological structure, and distance to the nearest spring.

The OLS results also indicated that the relationship between some or perhaps all of the explanatory variables and the dependent variable are non-stationary across the study area. Hence, GWR emerged as being more appropriate for analyzing those relationships because it has the capability of capturing the spatial non-stationarity of the influencing factors. GWR improved the model and explained 86% (better than OLS=57%) of the sinkhole density variability. The GWR model coefficient values for each explanatory variable provide visual insight into the influence of these variables on localized sinkhole density and patterns, and the values can be used to provide an objective means of parameter weighting in models of sinkhole susceptibility or hazard mapping/zoning.

Due to paucity of data, insufficient data form and model criteria, there are some potential influencing factors which were not included in the model (this may include falling or rising depth-to-groundwater, soil type, geochemical processes e.t.c). The OLS and GWR models were able to explain only 57% and 86% of the processes responsible for the formation of mapped sinkholes, respectively. Therefore further research incorporating more data with better resolution is recommended to improve the model.

REFERENCES

1. Arzu Erener, H. Sebnem B, Düzgün, 2010, Improvement of statistical landslide susceptibility mapping by using spatial and global regression methods in the case of More and Romsdal (Norway). *Landslides* (2010) 7:55–68, DOI 10.1007/s10346-009-0188-x.

2. Atkinson, P.M., German, S.E., Sear, D.A. and Clark, M.J., 2003, Exploring the relations between river bank erosion and geomorphological controls using geographically weighted logistic regression, *Geographical Analysis*, 35, (1), pp.58-82.

3. Blachowski. 2016, Application of GIS spatial regression methods in assessment of land subsidence in complicated mining conditions: case study of the Walbrzych coal mine (SW Poland). *Nat Hazards* DOI 10.1007/s11069-016-2470-2.

4. Brezinski, D.K., 2004, *Stratigraphy of the Frederick Valley and its Relationship to Karst*, Rep. No. 75, Annapolis: Maryland Department of Natural Resources.

5. Brook G.A, Allison T.L., 1986, Fracture mapping and ground susceptibility modeling in covered karst terrain—the example of Dougherty County, Georgia. In: *Land subsidence*, IAHSAISH Publication vol 151, pp 595–606.

6. Brundson C, Charlton M, Fotheringham S, 1996, Geographically weighted regression: a method for exploring spatial non stationarity. *Geogr* Anal 28:4

7. Brunsdon C, Fotheringham S, Charlton M., 1998, Geographically Weighted Regression- modelling spatial non-stationarity. *Journal of the Royal Statistical Society: Series D (The Statistician)* 47: 431–443. doi: 10.1111/1467-9884.00145.

8. Carbonel D, Rodríguez V, Gutiérrez F, et al. 2014, Evaluation of trenching, ground penetrating radar (GPR) and electrical resistivity tomography (ERT) for sinkhole characterization, *Earth Surf. Process. Landforms*, Vol. 39, 214–227.

9. Chalikakis, K., Plagnes, V., Guerin, R., et al., 2011, Contribution of geophysical methods to karst-system exploration: an overview, *Hydrogeology Journal*, 19: 1169–1180.

10. Charlton M, Fotheringham S, 2009, Geographically weighted regression. *White paper. National Centre for Geocomputation*, National University of Ireland Maynooth.

11. Doctor D, Doctor K., 2012, Spatial analysis of geologic and hydrologic features relating to sinkhole occurrence in Jefferson County, West Virginia. *Carbonates and Evaporites*, 27(2): 143–152.

12. Drake J.J, Ford D.C., 1972, The analysis of growth patterns of two generation populations—the examples of karst sinkholes. *Can Geogr* 16:381–384.

13. Environmental Systems Resource Institute (ESRI), 2014, *How OLS regression works*: Electronic document, available at http://resources.arcgis.com/en/help/main/

14. Environmental Systems Resource Institute (ESRI), 2014, *Interpreting OLS results*, :Electronic document, available at http://resources.arcgis.com/en/help/main/

15. Fellow L.D., 1970, *Geology of Galloway Quadrangle Greene County Missouri*, Missouri Geological Survey and Water Resources, pp 3-14.

16. Fotheringham, A.S., and Brunsdon, C., 1999, Local Forms of Spatial Analysis, *Geographical Analysis*, 31 (4), pp. 340–358.

17. Fotheringham A.S, Brunsdon C, Charlton M., 2002, *Geographically weighted regression—the analysis of spatially varying relationships*. Wiley, Chichester.

18. Galve P, Gutiérrez F, Remondo J, et al. 2009, Evaluating and comparing methods of sinkhole susceptibility mapping in the Ebro Valley evaporite karst (NE Spain), *Geomorphology*, v. 111, 160-172.

19. Gutiérrez, F., 2010, *Hazards associated with karst. In Geomorphological Hazards and Disaster Prevention*, Alcántara-Ayala I, Goudie A (eds). Cambridge University Press: Cambridge; 161–173.

20. Gutiérrez-Santolalla, F., Gutiérrez-Elorza, M., Marín, C., Desir, G., Maldonado, C., 2005b, Spatial distribution, morphometry and activity of La Puebla de Alfindén sinkhole field in the Ebro River valley (NE Spain) applied aspects for hazard zonation. *Environmental Geology* 48, 360–369.

21. Hyatt, J., Wilkes, H., Jacobs, P., 1999. Spatial relationship between new and old sinkholes in covered karst, Albany, Georgia, USA. In: Beck, B.F. (Ed.), *Hydrogeology and Engineering Geology of sinkholes and Karst.* Proceedings of the 7th Multidisciplinary Conference on Sinkholes and the Engineering and Environmental Impacts of Karst. Harrisburg, Pennsylvania, USA, pp. 37–44.

22. Kalogirou, S., and Hatzichristos, T., 2007, A spatial modelling framework for income estimation, *Spatial Economic Analysis*, 2, 3, p. 297–316.

23. Kaufmann J., 2008, A Statistical Approach to Karst Collapse Hazard Analysis in Missouri. *Sinkholes and the Engineering and Environmental Impacts of Karst* (2008): pp. 257-268.

24. Kemmerly, P.R., 1982. Spatial analysis of a karst depression population: clues to genesis. *Geological Society of America Bulletin* 93, 1078–1086.

25. Liao, Q., Li, M., Chen, Z., Shao, Y., Yang, K., 2010, Spatial simulation of regional land use patterns based on GWR and CLUE-S model, *Proceedings of the 18th International Conference on Geoinformatics*, Beijing, China, 18-20 June 2010, pp. 1-6, DOI: 10.1109/GEOINFORMATICS.2010.5567963.

26. Missouri Department of Natural Resources, 2016, *Missouri Geological Survey* Geosciences Technical Resource Assessment Tool (*GeoSTRAT*): Electronic geospatial data, available at https://dnr.mo.gov/

27. Missouri Spatial Data Information Service (MSDIS), 2016, Electronic geospatial data, available at http://msdis.missouri.edu/

28. Ndiath, MN, Cisse, B., Ndiaye, J.L., Gomis, J.F., Bathiery, O., Dia, A.T., Gaye, O., Faye, B. (2015). Application of geographically-weighted regression analysis to assess risk factors for malaria hotspots in Keur Soce health and demographic surveillance site. *Maleria Journal*, 14:463.

29. Orndorff R.C, Weary D.J, Lagueux K.M., 2000, Geographic information systems analysis of geologic controls on the distribution of dolines in the Ozarks of south-central Missouri, USA. - *Acta Carsologica* 29/2, 161-175, Ljubljana.

30. Rogers, J. David, 1997, Spatial Geologic Hazard Analysis in Practice: in Spatial Analysis in Soil Dynamics and Earthquake Engineering, ed. J. David Frost, *ASCE Geotechnical Special Publication* No. 67, pp. 15-28.

31. Waltham, T., Bell, F., Culshaw, M.G., 2005, Sinkholes and Subsidence; Karst and cavernous rocks in engineering and construction. Chichester, UK: Praxis, *Springer* 382pp.

32. Windle M.J.S, Rose G.A, Devillers R and Marie-Josée F., 2010. Exploring spatial non-stationarity of fisheries survey data using geographically weighted regression (GWR): an example from the Northwest Atlantic. *ICES J. Mar. Sci*. 67 (1): 145-154. doi: 10.1093/icesjms/fsp224.

33. Zhou, W., Beck, B.F., and Adams, A.L., 2003, Application of Matrix Analysis in Delineating Sinkhole Risk Areas along Highway (I-70 near Fredrick, Maryland), *Environmental Geology*, No. 44, pg. 834-842.

II. ERT-BASED INVESTIGATION OF A SINKHOLE IN GREENE COUNTY, MISSOURI

Shishay T. Kidanu* , Evgeniy V. Torgashov, Aleksandra V. Varnavina, Neil L. Anderson

Department of Geosciences and Geological and Petroleum Engineering, Missouri University of Science and Technology, Rolla, MO 65409, USA.

* Correspondence: Email: stkq7f@mst.edu; Tel: +1 573 578 0645

ABSTRACT

Investigating sinkhole morphology and formation mechanisms is key to understanding their long term impact and susceptibility to development, and aids in the design of effective mitigation measures. In this study, ERT (electrical resistivity tomography), MASW (multichannel analysis of surface waves) and borehole data were used to image the subsurface morphology of an active sinkhole in Greene County, Missouri. The study reveals that the sinkhole developed along a natural surface drainage pathway above a pervasively fractured limestone. The subsurface image of the sinkhole depicts a zone of near-vertical water seepage and soil piping. Based on the nature of the overburden material, and the morphology and current/past surface expression of the sinkhole, it is concluded that the sinkhole is predominantly a cover subsidence type of sinkhole. However, it is possible that minor cover collapse occurred locally and in an area slightly to the north of the current active sinkhole.

Key words**:** sinkhole; ERT; MASW; piping; borehole control; subsidence

1. INTRODUCTION

Greene County, Missouri, is part of the Ozarks physiographic region and is known for its karst terrain. Karst terrain forms in carbonate and evaporitic rocks, primarily by dissolution and is typically characterized by numerous sinkholes, losing streams (swallow holes), springs, caves, and other related features. Because of this, karst areas are one of the most challenging environments in terms of groundwater, engineering and environmental issues [1]. Sinkholes are one of the most common karst structures in the world [2] and constitute a major hazard in karst areas [3, 4].

Greene County Missouri is known for the presence of karstic features such as caves, springs and, more importantly, sinkholes [5]. It is reported that more than 2500 sinkholes and 245 caves have been identified in Greene County (Greene County Comprehensive Plan, page 52, 2007). As stated by Carbonel et al. in [6], catastrophic collapsing sinkholes may lead to injury, fatalities and cause significant damage to infrastructure. For example, the sinkhole that occurred in Nixa, Missouri, on August 13, 2006, swallowed a car, the garage it was parked in, and part of the adjoining house [7].

Geology, hydrology, and anthropogenic factors have an impact on the formation of sinkholes [7–9]. Hence, an understanding of the interaction between these factors assists in determining where and how a sinkhole may form. Moreover, the investigation of the formation mechanism and sinkhole morphology allows for design of applicable mitigation measures. Investigation of existing sinkholes is necessary from an engineering standpoint to locate and characterize the source of water, seepage/piping pathways, voids (if present) and variable depth to top of rock. As stated by Gutiérrez in [10], effective sinkhole investigation should integrate a variety of investigative approaches that include geological,

geophysical, and geomorphological analysis. The author's perspective is that any sinkhole can be mitigated using appropriate engineering technologies if the flow of piping water is effectively cut-off.

Geological analysis and geophysical methods can assist in characterizing sinkhole morphology, evolution and formation mechanisms, while geomorphological methods assist in the understanding of recent sinkhole activity and human influences [2]. Geophysical methods are often particularly useful as there is usually a good contrast between the physical properties of the sinkhole fill, which consists of either water, air, or soil, and the surrounding less disturbed strata. Geophysical methods that are commonly used for sinkhole investigation include seismic reflection and refraction [11], gravimetry [12], ground-penetrating radar [13, 14], electrical resistivity tomography [15–18], and multichannel analysis of surface waves [19, 20].

Electrical resistivity tomography (ERT) is routinely used in Missouri to image the shallow subsurface in karst terrain because undisturbed soil, carbonate rock, clay in-fill, and air-filled cavities are generally characterized by very high resistivity contrasts [5]. Multichannel analysis of surface waves (MASW) is also often a very appropriate method for sinkhole investigation, because variations in shear-wave velocity can be used to differentiate between various types of unconsolidated soils and bedrock [21].

In this research ERT and MASW techniques were employed together with a confirmatory boring to effectively characterize the subsurface morphology of an active sinkhole, hereafter referred to as Sinkhole_1. Moreover, historical maps were analyzed to reveal the evolution of the karst feature and land use changes. Analyses suggest the sinkhole developed along a natural north-south surface drainage pathway. Furthermore, the

subsurface structure of the sinkhole depicts a vertical zone of moisture flow and associated soil piping. From the nature of the overburden material and the characteristics of the sinkhole, it is concluded that the sinkhole is predominantly a cover subsidence sinkhole (gradual subsidence) based on the sinkhole classification system described by Waltham et al. in [22]. Historical photographs suggest that cover collapse could have occurred in an area slightly to the north of the current active sinkhole.

2. LOCATION AND GEOLOGY OF STUDY AREA

Sinkhole_1, is located in Greene County, Missouri (Figure 1). The geology of Greene County comprises thick Mississippian-age limestones and cherty limestones underlain by Ordovician and Cambrian-aged strata (Table 1). Greene County lies on the western side of the Ozark Uplift and the rock layers regionally dip gently towards the west with minor faulting and folding.

The Mississippian age Burlington-Keokuk Limestone is the dominant bedrock exposed in the study area (Figure 2). In this bedrock, layers of limestone are interbedded with thin layers of chert and the presence of chert nodules within limestone layers.

The Burlington-Keokuk Formation is up to 270ft (82.3m) thick [23] but varies in thickness from place to place due to erosion. The limestone is a light gray, coarsely crystalline, and nearly pure calcite which is highly susceptible to solution. Uneven dissolution of this formation has resulted in highly irregular bedrock-overburden interface [24]. This limestone bedrock is mainly characterized by the formation of prominent knobs (pinnacles) of bedrock bounded by deep troughs (grikes) caused by dissolution in pre-existing fractures. The thickness of residuum is highly variable, in many areas stream

erosion has removed the residuum and rock is at or very near to the surface, whereas in other areas it reaches to a thickness of about 40ft (12.2m) [25].

The limestone bedrock in Greene County was subjected to tectonic forces and has undergone some structural deformations during the Ouachita Orogeny. Orndorff in [26] has mentioned that the geological structures formed from this deformation appear to have controlled the development of karst. Generally, the faults in the study area are oriented northwest and northeast [27]. Joints are common structural features, similar to faults, where lateral and vertical displacements have not occurred. McCracken in [27], states that the bedrock in the study area is characterized by two nearly orthogonal joint sets that exhibit general strike orientations: N 20 º W, and N 60 º E and with vertical dipping.

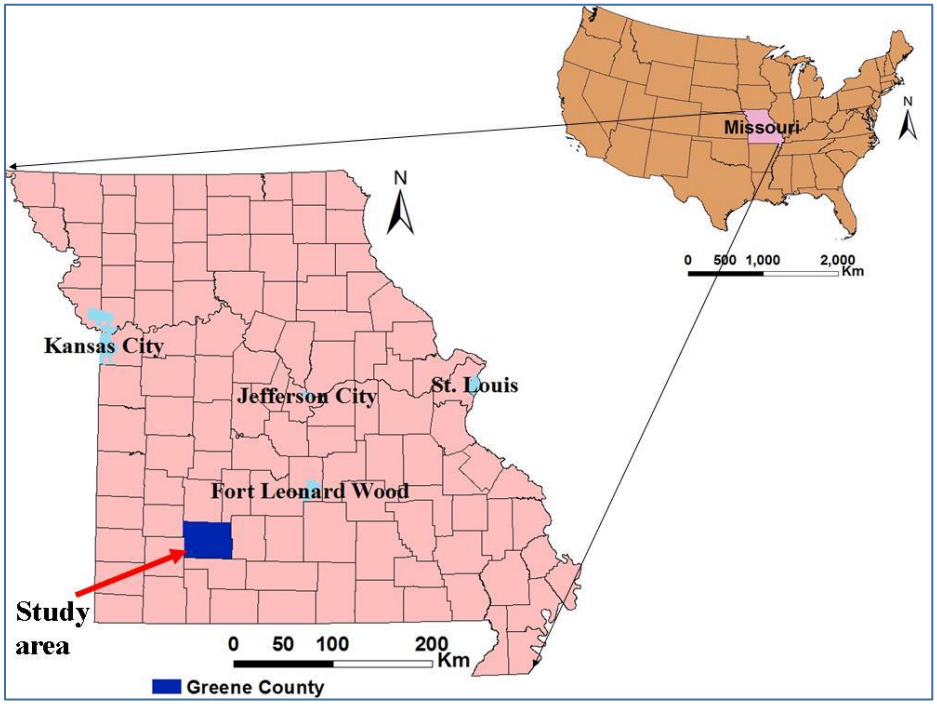

Figure 1. Location Map of the study area: the blue color region represents Greene County, Missouri.

Table 1. Geologic and stratigraphic units in Greene County [23].

System	Series	Group	Formation		Thickness (ft)
Mississipian	Osagean		Burlington-Keokuk Formation		150-270
			Elsey Formation		25-75
			Reeds-Spring Formation		125
			Pierson Formation		90
	Kinkerhookian	Chouteau	Northview Formation		5-80
			Compton Formation		30
Ordovician	Canadian		Cotter Formation		600
			Jefferson-City Formation		
			Ruobidoux Formation		150
			Gasconade Formation	Upper Gasconade Dolomite	350
				Lower Gasconade Dolomite	
				Gunter Sandstone Member	25
Cambrian	Upper		Eminence Formation		500
			Potasi Formation		
		Elvins	Derby-Doerun Formation		
			Davis Formation		150
			Bonneterre Formation		200
			Lamotte Formation		150
Precambrian	Crystalline rock				

Karst features are prevalent almost throughout Greene County. The Burlington-Keokuk Limestone has been extensively affected by solution process resulting in the formation of numerous karst features: caves, springs, sinkholes, losing streams, cherty clay residuum, etc. As stated by Ismail and Anderson in [5], the sinkholes are formed when carbonic acid from atmospheric carbon dioxide, present in rainwater, percolates downwards into the subsurface and dissolves carbonate bedrock, enlarging fractures and joints into cavities that in most cases were in-filled with piped fine-grained soil as they developed, resulting in gradual subsidence at the surface.

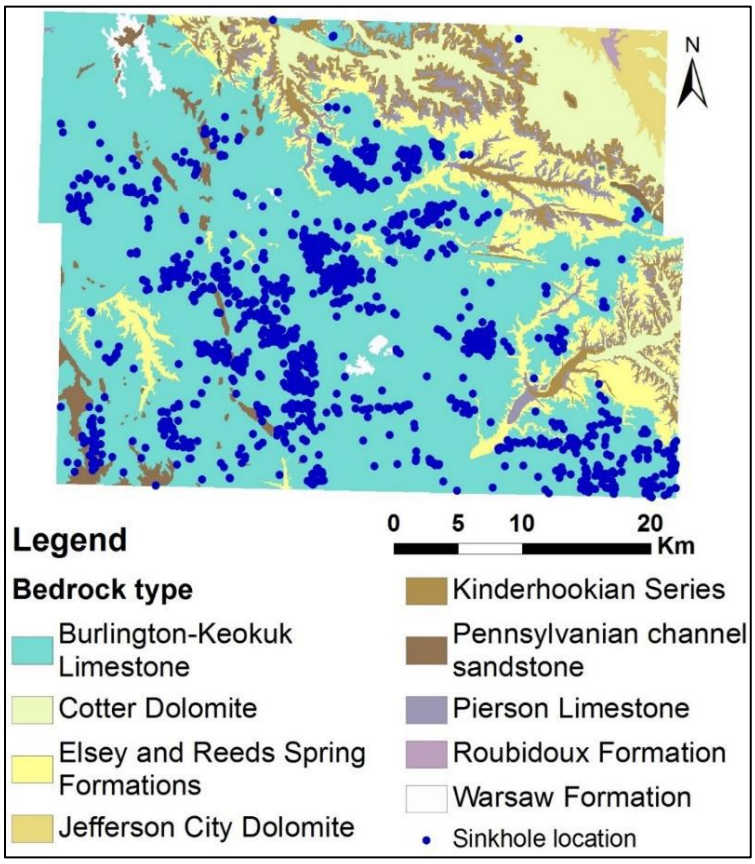

Figure 2. Geological map of Greene County, Missouri (Esri data source: Missouri Geological Survey GEOSTRAT system, Sept 2015).

3. ASSESSMENT OF THE SINKHOLE

3.1. AERIAL PHOTOS

An aerial photograph from 1960 and a series of historical google earth images (Figure 3) were analyzed to reveal the evolution of Sinkhole_1, anthropogenic factors and land use changes. The 1960 aerial photo on the top left of Figure 3 shows a north-south elongated feature which is a row of trees along a natural north-south surface drainage pathway in the middle of a farmer's field. To the north of the row of trees, there is a small

surface depression. This suggests that Sinkhole_1 developed at this location originally as a result of the localized ponding of surface water immediately to the north of the zone of dense vegetation. The ponded water and piped fine-grained sediment percolated into the subsurface through the soil and underlying pervasively fractured limestone. The piping of soil lead to surface subsidence and the enlargement of the sinkhole over time.

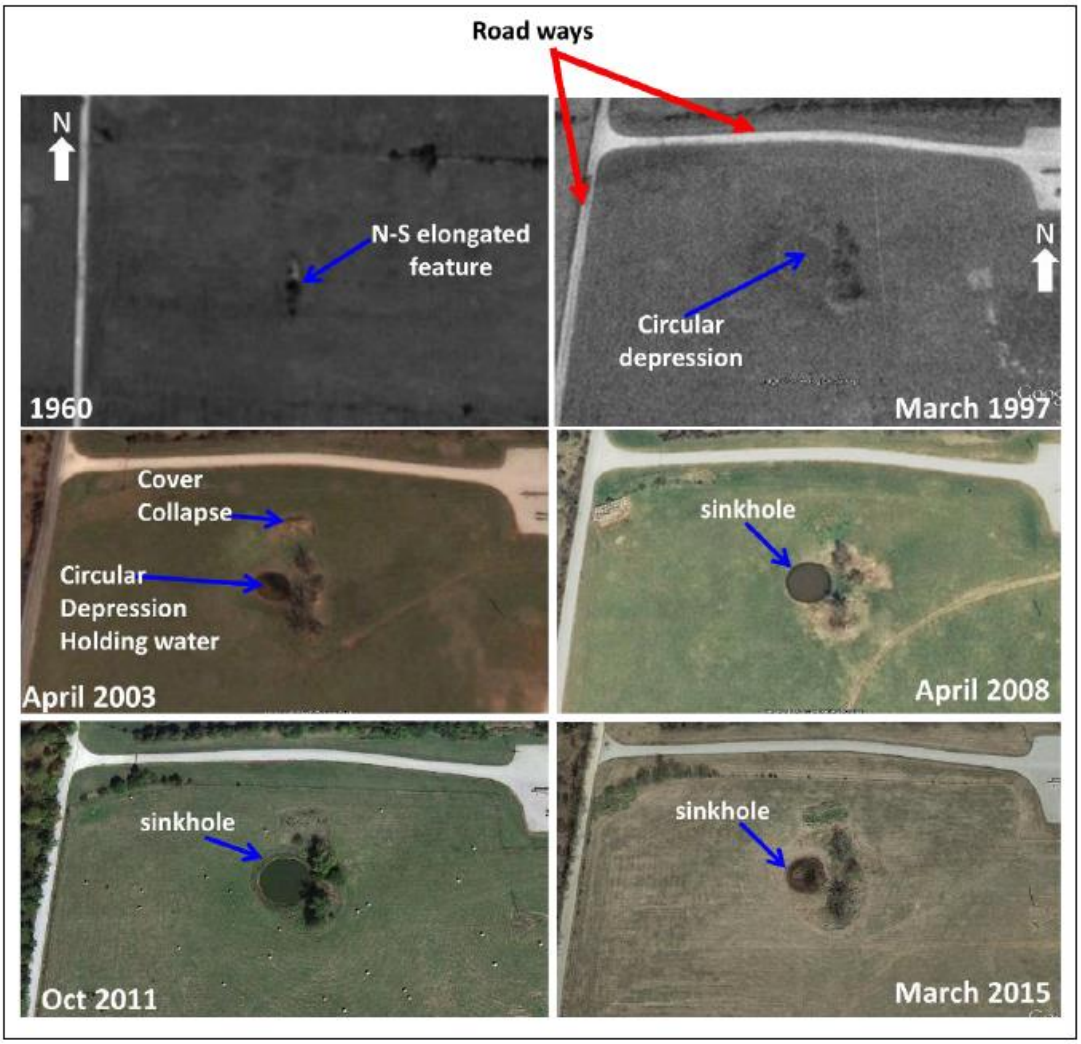

Figure 3. Historical Aerial photos of Sinkhole_1; the paved road ways can give an idea about the scale of the images.

The second image, a Google Earth® image from March 1997, shows a well-defined circular depression, immediately west of the row of trees imaged in the 1960 photograph. The circular depression is the surface expression of the Sinkhole_1 in 1997. The sinkhole appears to have migrated to the west as a result of the broadening of the surface expression of the original area of subsidence. The observation that the zone subsidence is covered by vegetation and not characterized by scarp features indicates Sinkhole_1 is predominantly a cover subsidence type of sinkhole. The Google Earth® image from April 2003, shows a small surface depression to the north of the main circular depression. The steep angle and the lack of vegetation/grass cover on the scarp in the collapse feature suggest that this collapse may have occurred relatively abruptly. It is possible that this depression is a localized cover collapse feature. Cover collapse is a typical feature of sinkhole development in cohesive soils where the covering sediments contain significant amount of clay. The sediments spall into a cavity and as spalling continues, the cohesive covering sediments form a structural arch and eventually the cavity breaches the ground surface, resulting in sudden and dramatic collapse usually with steep angle scarps.

The series of historical images indicate that Sinkhole_1 is not an instantaneous collapse type of sinkhole; rather it appears to have developed gradually and evolved over time. Sinkhole_1 is therefore classified as cover subsidence. It appears to have initiated about the time the 1960 photograph was taken.

3.2. BOREHOLE CONTROL

One borehole (BH1) was drilled to facilitate the correlation of the ERT profiles to the actual subsurface geology. The drilling was advanced to the bedrock surface using 8.5 inch (21.6cm) O.D. hollow-stem augers and bedrock was cored using HQ core barrels.

The borehole (BH1) was drilled along ERT profile T13 and ties at 97.5m mark on the profile (Figure 5 and 6a). It was drilled to a depth of 30m below ground surface. The first 2m comprises red clay residuum with chert, with brown silty loam with chert from 0 - 1.1m; 1.1m - 1.8m comprises red silty high plasticity clay, and finally 1.8m - 2m reveals low plasticity clay. Underlying the residual soil is Burlington-Keokuk Limestone, characterized, in core specimens, by numerous horizontal fractures. The rock quality was found to be fair to excellent.

The decomposition of the beds of limestone and chert formed a highly ferruginous deposit of clay mixed with broken and decomposed chert. The broken and decomposed chert gives more porosity to the residual clay soil. Furthermore, the high iron content of the ferruginous clay residuum causes flocculation and form blocky aggregates resulting in increased porosity of the soil. Therefore, as a result of the presence of chert fragments and the flocculated clay structure, the residuum clay soil has higher permeability than expected from a more uniform clay soil. From the borehole samples it is evident that the clay content increases with depth, and this supports the idea that there is piping of fine grained soils.

3.3. MULTICHANNEL ANALYSIS OF SURFACE WAVES (MASW)

Multichannel analysis of surface waves (MASW) data were acquired in proximity to Sinkhole_1 and along west-east oriented ERT profiles (Figures 4 and 5). A 24 channel geophone array connected to a seismograph is used to record the seismic data. As presented in Figure 5, six MASW profiles (MASW1, MASW2, MASW3, MASW4, MASW5 and MASW6) were generated and used to verify and constrain the interpretation of the ERT profiles. The NEHRP (National Earthquake Hazard Reduction Program) site classification chart for different geological material, as published in 2000 by the International Building

code, provides a basis for the classification of subsurface materials based on their shear wave velocity values. Based on this chart and the borehole control, the shear wave velocity of soil is generally less than 1200feet/sec (366m/sec). An example dispersion curve and corresponding 1-D shear wave velocity profile from MASW5 is presented as Figure 4.

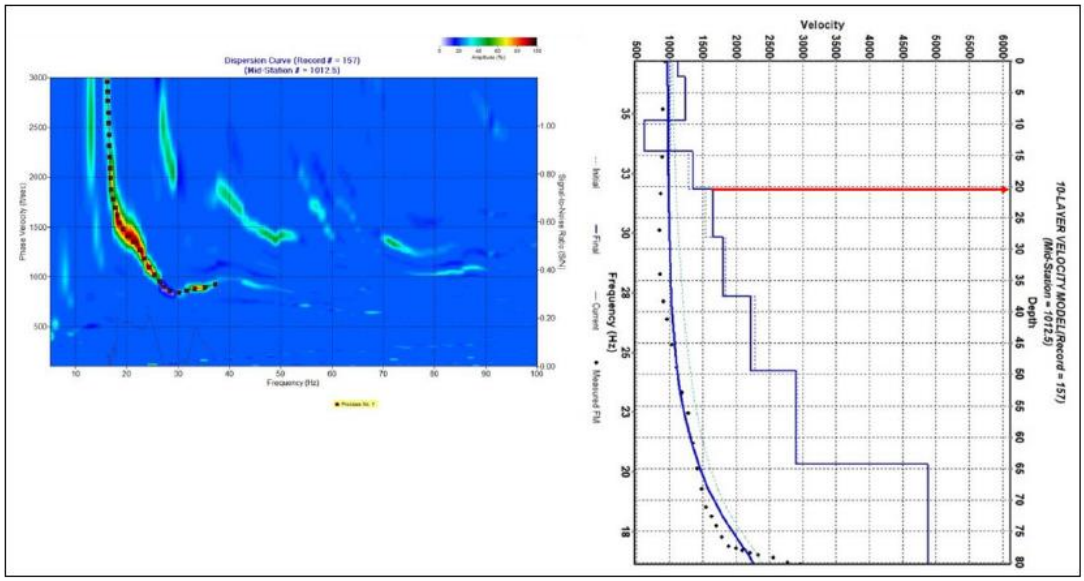

Figure 4. A dispersion curve (left); and 1-D shear wave velocity profile (right) of MASW5 presented as sample; acquisition parameters used are 10ft (3.05m) off-set, 5ft(1.52m) geophone spacing, and aligned E-W. Red color arrow indicates interpreted depth to top of rock.

3.4. ELECTRICAL RESISTIVITY TOMOGRAPHY (ERT)

Sixteen west-east oriented 2D electrical resistivity tomography (ERT) profiles were taken at the site with the intent of imaging and characterizing the shallow subsurface in the vicinity of Sinkhole_1. The ERT profiles were acquired along sixteen west-east oriented

traverses spaced at 6.1m (20ft) intervals. The traverses are labeled T1, T2, T3, to T16 (Figure 5). Each 2D-ERT profile extends to a maximum depth of 36.5m (120ft). The west-east direction was selected as it is nearly perpendicular to major joints and regional geological structures in the study area, which have a general approximately north-south orientation. ERT data were acquired using an AGI R-8 Supersting multi-channel and multi-electrode resistivity system with 168 electrodes spaced at 1.52m (5ft) intervals and using a dipole-dipole electrode array.

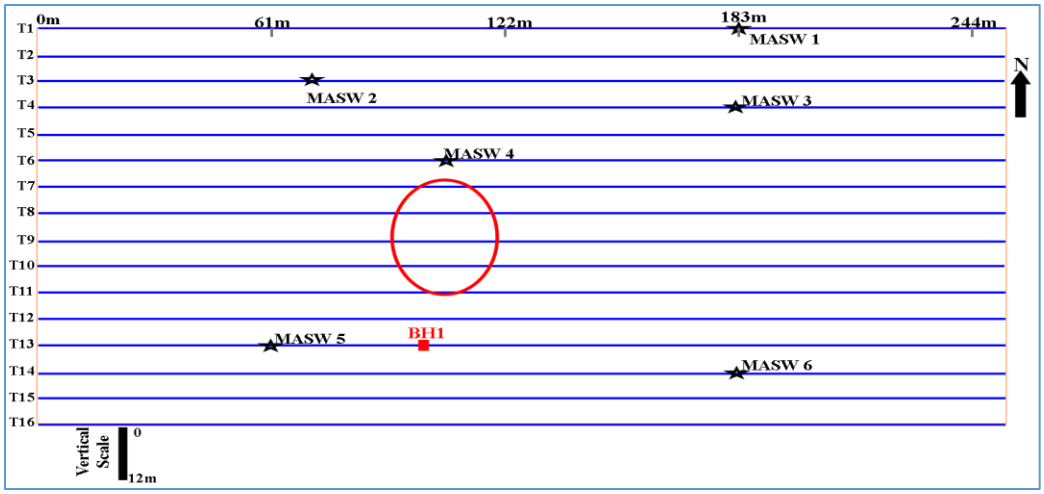

Figure 5. Alignment and location of acquired geophysical data and borehole control: West-east oriented blue lines represent ERT traverses (254.5m long each). The red color circle represents the approximate location of the surface expression of Sinkhole_1.

The borehole control and MASW interpretations were superposed on the respective ERT profiles to help verify the interpretations of the electrical resistivity images. Based on the borehole data (BH1) (Figure 6a), the top of weathered rock corresponds approximately

to the 125 ohm-m resistivity contour interval on ERT profile T13. Therefore, the resistivity contour value of 125 ohm-m is interpreted as the top of weathered rock on all of the other ERT profiles. Further, BH1 overlain (superposed on T13; Figure 6a) indicates that the zone of relatively low electrical resistivity (Zone A) is not a soil/water filled cavity, but rather fractured and weathered rock with fair to good quality. Therefore, the relatively low resistivity values (less than 125 ohm-m) are attributed to the presence of moisture and/or clay filled fractures. Hence, Zone A is interpreted as a moist fractured rock with some clay infilling fractures. MASW5 ties ERT T13 at 61m mark (Figure 6). The "resistivity" top of weathered rock at the MASW5 location is estimated to be 20ft (6.1m). The 1-D shear wave velocity profile in MASW5 (Figure 6b) shows an abrupt increase of velocity from 1300ft/sec (396m/sec) to 1650ft/sec (503m/sec) at a depth of 20.5ft (6.2m). This increase presumably marks the boundary between dense residual soil and the top of weathered rock and is interpreted as the "acoustic" top of rock. The additional acquired MASW data also correlate with ERT profiles, in terms of estimated depths to top of rock. Figure 7a shows MASW1 tied to the ERT profile T1 at 183m mark; the "resistivity" and "acoustic" top of weathered rock are 2.4m and 2.1m respectively. In Figure 7b, Zone B has very low electrical resistivity (less than 125 ohm-m), but its average shear wave velocity in MASW4 is about 1800ft/sec (549m/s). Similarly, the low resistivity zone (Zone C) in Figure 7c, is characterized by a shear wave velocity ranging from 1450ft/sec (442m/sec) to 1800ft/sec (549m/sec). These values of shear wave velocity are consistent with that of fractured rock. Moreover, strata with comparable resistivity values and similar geological conditions encountered in the borehole was fractured rock (Figure 6a). Hence the most plausible

interpretations of zones B and C is that they are zones of fractured rock probably with moist clay infill.

Based on control available, the following interpretational guidelines were established: moist soils are characterized by resistivity values of less than 125 ohm-m; dry soils by resistivity values greater than 125 ohm-m; moist weathered and/or fractured rock by resistivity values less than 600 ohm-m; moist fractured rock with moist piped clay/soil-fill by resistivity values less than 125 ohm-m; and drier, possibly less weathered rock by resistivity values greater than 600 ohm-m. Large air filled cavities should be characterized by very high resistivity values, but dependent on the conductivity of the surrounding material and depth/size/shape of the void. The ERT data acquired at this study indicated that the active sinkhole is not underlain by any substantive air-filled cavities. Four ERT profiles crossing the sinkhole (T7, T8, T9, and T10), with interpreted depths to moist weathered rock and depths to drier, possibly less weathered rock, are shown as Figure 8.

4. PROMINENT JOINT SET

A linear, north-south oriented zone of relatively low resistivity that extends through Sinkhole_1 is readily identified on Figure 9. This linear feature (labeled as joint set 1 in Figure 9) could be a zone of more intense fracturing (i.e. north-south trending joint set). Alternatively, in as much as the zone underlies a natural north-south trending surface drainage pathway, this zone of low resistivity could simply be the result of moisture with piped fines percolating into the subsurface over an extended period of time presumably with some attendant solution-widening. In addition to the prominent north-south oriented linear feature (joint set 1), other roughly linear trends of low resistivity anomalies with

different orientations are also observed in Figure 9. These anomalies are not visually prominent enough and also not well defined linear features to be interpreted as joint sets. However, their general linear trend gives an insight into the possibility of presence of other joint sets or lineaments.

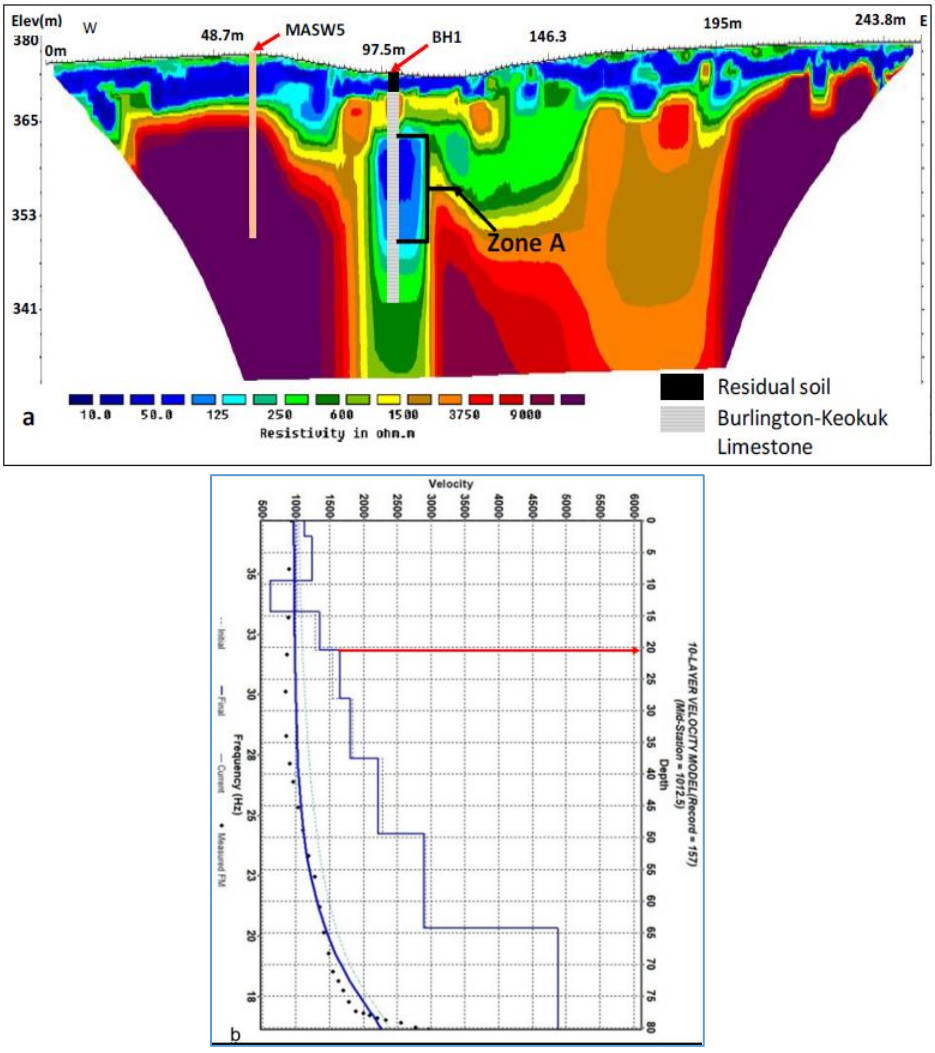

Figure 6. (a) ERT profile T13 with overlaid MASW5 and borehole (BH1). MASW5 tied T13 at the 61m mark; BH1 ties T13 at the 100m mark; (b) MASW5 1-D shear wave velocity profile. MASW depth to top of weathered rock ("acoustic" top of rock) is 20.5ft (6.2m). Red color line on Figure 6b indicates interpreted depth to top of rock.

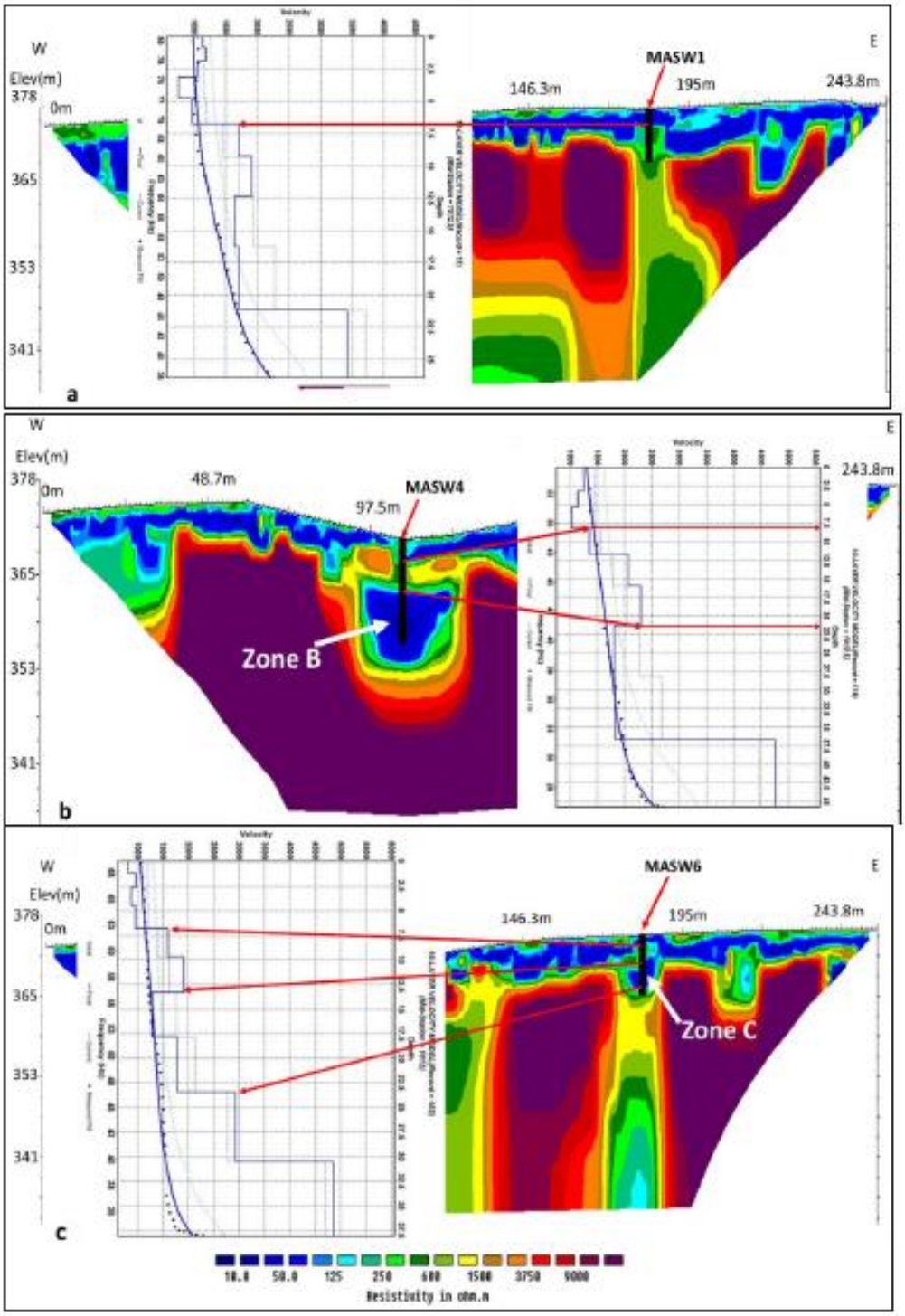

Figure 7. Correlation of the interpretation of ERT and MASW. The acquisition parameters: Offset, geophone spacing and alignment used are as follows in MASW1, 10ft (3m), 2.5ft (0.76m), N-S); in MASW4, 10ft (3m), 5ft (1.52m), E-W), and in MASW6, 10ft (3m), 5ft (1.52m), N-S).

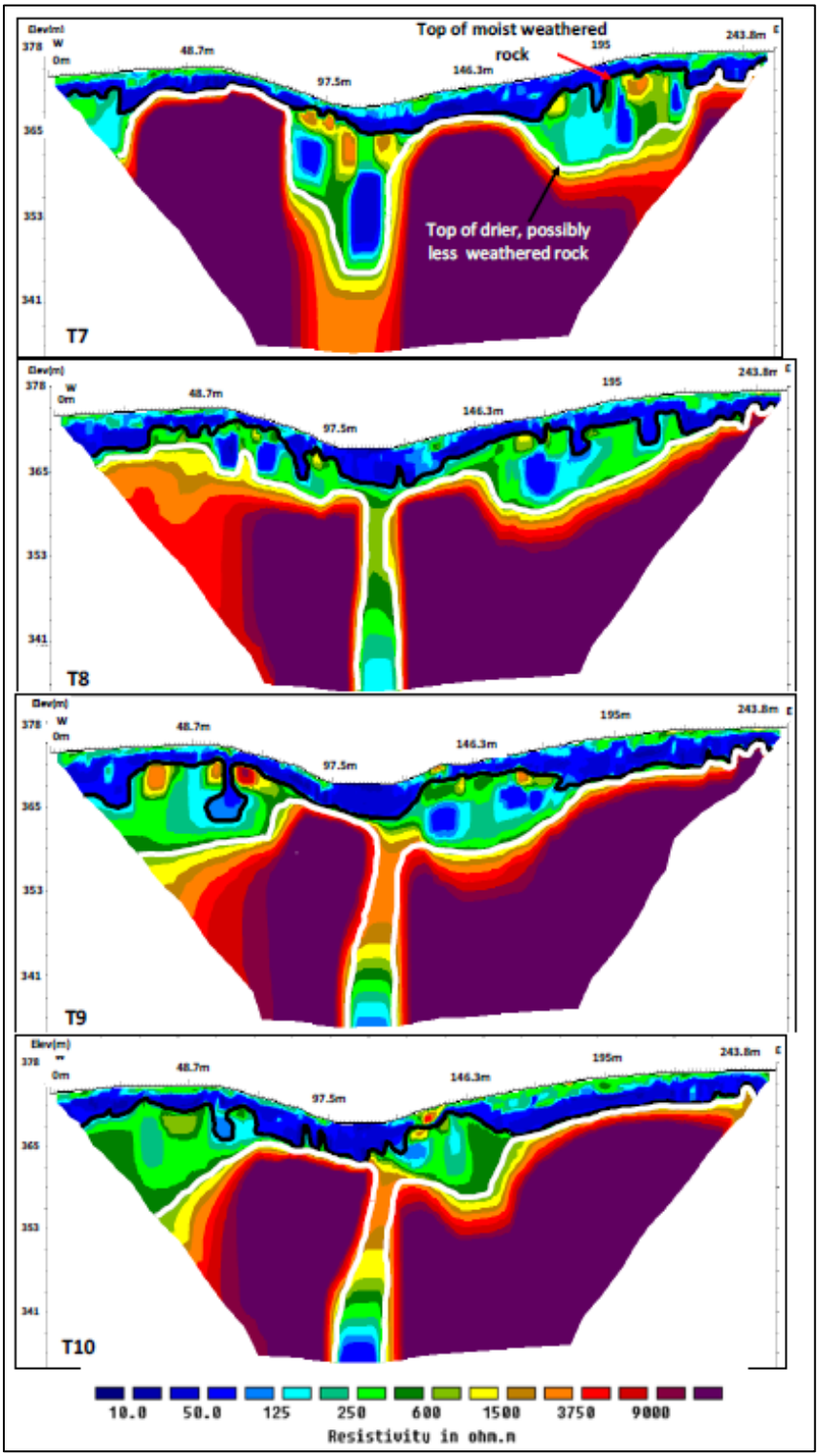

Figure 8. 2D-ERT profiles (T7, T8, T9 and T10) with interpreted top of moist weathered rock and top of drier, possibly less weathered rock. The labels given for the white and black lines in T7 are the same for T8, T9 and T10.

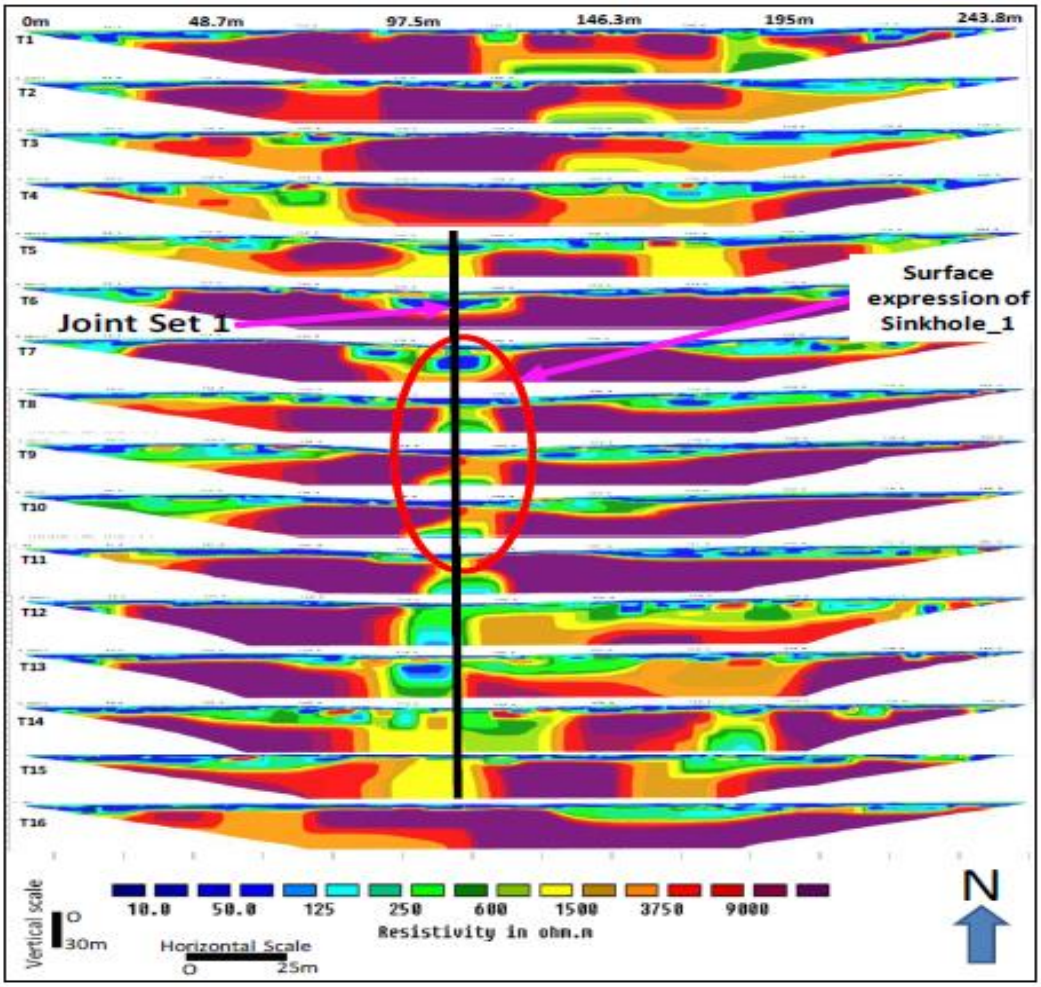

Figure 9. Parallel alignment of 16 W-E oriented 2D-ERT profiles with an approximate location of surface expression of Sinkhole_1 (in red). Each ERT profile has a length of 835ft (254.5m). Horizontal scale and vertical scale are not the same.

5. GEOLOGICAL MODEL OF SUBSURFACE STRUCTURE OF THE SINKHOLE

The interpreted 2D-resistivity profiles (T7, T8, and T9) together with information from the borehole log were used to generate geological models depicting the subsurface structure of Sinkhole_1 (Figure10.T7, T8 and T9). Sinkholes develop as a result of

interrelated processes, including bedrock dissolution, rock collapse, soil down-washing/piping and soil collapse. Any one or more of these processes may lead to the development of a sinkhole. The bedrock structure underneath the surface expression of Sinkhole_1 (Figure 10) does not show any sign of major rock collapse. In all the three images (Figure 10), there are zones interpreted as moist, intensely weathered rock with clay fill at various depths beneath and in proximity to the surface expression of Sinkhole_1. This implies that the major process involved in the development of the sinkhole is downward piping of fine-grained sediments, which fill existing and/or developing fractures. As mentioned in previously, the clay residuum has chert fragments and is not as cohesive as it would be expected from a more uniform clay soil. Hence, it is concluded that the sinkhole development involved predominantly a cover subsidence processes, possibly with minor localized cover collapse. From the subsurface structure and surface expression of the sinkhole, plus the nature of the overburden material, Sinkhole_1 is classified as predominantly a cover subsidence sinkhole.

6. CONCLUSION AND RECOMMENDATION

Two-dimensional electrical resistivity profiles were acquired across and in proximity to a sinkhole in Greene County, Missouri. The acquired 2-D resistivity data were processed as 2-D resistivity profiles and the interpretation was supported by a complementary MASW and borehole control data.

The study shows that Sinkhole_1 developed along a natural surface water drainage pathway, possibly above a north-south oriented joint set, and is characterized by a visually prominent zone of low resistivity.

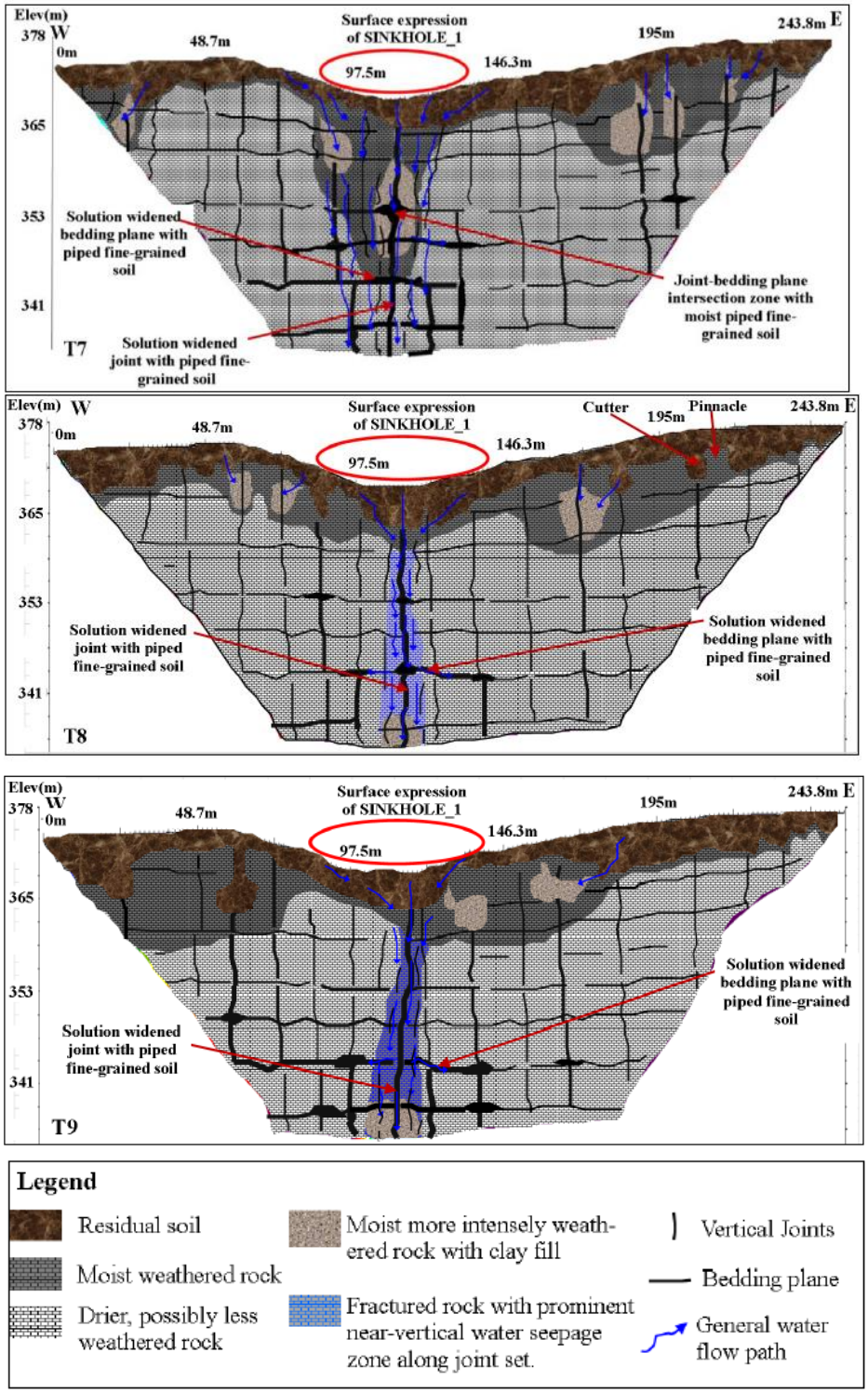

Figure 10. Geological model of the subsurface structure of Sinkhole_1, reconstructed from interpreted 2D-ERT images; T7, T8, T9 and borehole control and MASW. Horizontal and vertical scale are not the same.

The relatively low resistivity values are due to vertical water seepage and the associated piping fine grained soils primarily into preexisting fractures. This supports the principle that sinkholes develop in areas where water is ponded or temporarily retained and able to percolate into the subsurface. Thus a sinkhole can be mitigated using appropriate engineering technologies if the source of piping waters is shut-off.

REFERENCES

1. Chalikakis K, Plagnes V, Guerin R, et al. (2011). Contribution of geophysical methods to karst-system exploration: an overview, Hydrogeology Journal, 19: 1169–1180.

2. Festa V, Fiore A, Parise M, et al. (2012). Sinkhole evolution in the Apulian karst of southern Italy; a case study, with some considerations on sinkhole hazards. *Journal of Cave and Karst Studies*, v. 74, p. 137-147.

3. Waltham T, Bell F, Culshaw MG (2005). Sinkholes and Subsidence; Karst and cavernous rocks in engineering and construction. Chichester, UK: Praxis, Springer 382pp.

4. Gutiérrez F (2010). Hazards associated with karst. In Geomorphological Hazards and Disaster Prevention, Alcántara-Ayala I, Goudie A (eds). Cambridge University Press: Cambridge; 161–173.

5. Ahmed I, Neil A (2012). 2-D and 3-D Resistivity Imaging of Karst Sites in Missouri, USA. Environmental & Engineering Geoscience, Vol. XVIII, No. 3, August 2012, pp. 281–293.

6. Carbonel D, Rodríguez V, Gutiérrez F, et al. (2014). Evaluation of trenching, ground penetrating radar (GPR) and electrical resistivity tomography (ERT) for sinkhole characterization, Earth Surf. Process. Landforms, Vol. 39, 214–227.

7. Kaufmann J (2008). A Statistical Approach to Karst Collapse Hazard Analysis in Missouri. Sinkholes and the Engineering and Environmental Impacts of Karst (2008): pp. 257-268.

8. Galve P, Gutiérrez F, Remondo J, et al. (2009). Evaluating and comparing methods of sinkhole susceptibility mapping in the Ebro Valley evaporite karst (NE Spain), *Geomorphology*, v. 111, 160-172.

9. Doctor D, Doctor K (2012). Spatial analysis of geologic and hydrologic features relating to sinkhole occurrence in Jefferson County, West Virginia. Carbonates and Evaporites, 27(2): 143–152.

10. Gutiérrez F, Cooper HA, Johnson KS (2008) Identification, prediction and mitigation of sinkhole hazards in evaporate karst areas. Environ Geol 53:1007–1022.

11. Cook JC (1965) Seismic mapping of underground cavities using reflection amplitudes. Geophysics 30(4):527–538.

12. Ballard RF (1983) Cavity detection and delineation research. Report 5, Electromagnetic (radar) techniques applied to cavity detection. Technical Report GL, 83–1, pp 90.

13. Annan AP, Cosway SW, Redman JD (1991) Water table detection with ground-penetrating radar. In: Soc. Explor. Geophys (Annual International Meeting Program with Abstracts), pp 494–497.

14. Labuda TZ, Baxter AC (2001), Mapping karst conditions using 2D and 3D resistivity imaging methods, paper presented at the Symposium on the Application of Geophysics to Engineering and Environmental Problems (SAGEEP), Environ. and Eng. Geophys. Soc., Denver, Colorado.

15. Roth MJS, Mackey JR, Mackey C, et al. (2002). A case study of the reliability of multi-electrode earth resistivity testing for geotechnical investigations in karst terrains, Eng. Geol., 65, 225–232.

16. Zhou W, Beck BF, Adams AL (2002). Effective electrode array in mapping karst hazards in electrical resistivity tomography. Environ. Geol. 42:922–928.

17. Ahmed S, Carpenter PJ (2003). Geophysical response of filled sinkholes, soil pipes and associated bedrock fractures in thinly mantled karst, east-central Illinois. Environmental Geology, 44:705–716.

18. Lee R, Callahan P, Shelly B, et al. (2010). MASW Survey Identifies Causes of Sink Activity Along I-476 (Blue Route), Montgomery County, Pennsylvania. In: GeoFlorida 2010 Conference; Feb. 20-24.

19. Debeglia N, Bitri A, Thierry P (2006). Karst investigations using microgravity and MASW; application to Orleans, France. Near Surface Geophysics 4: 215–225.

20. Odum JK, Williams RA, Stephenson WJ, et al. (2007). Near-surface shear wave velocity versus depth profiles, Vs 30, and NEHRP classifications for 27 sites in Puerto Rico:USGS Open-File Report 2007-1174.

21. Waltham AC, Fookes PG (2005). Engineering classification of karst ground conditions. Speleogenesis and Evolution of Karst Aquifers, the Virtual Scientific Journal ISSN 1814-294X.

22. Vandike JE (1993) Groundwater level data for Missouri: Water year 1991-1992. Missouri Department of Natural Resources. Division of Geology and Land Survey. Water Resource Report No.42. Rolla, Missouri.

23. Fellow LD (1970). Geology of Galloway Quadrangle Greene County Missouri, Missouri Geological Survey and Water Resources, pp 3-14.

24. Hayes WC, Thomson KC (1973). Engineering and environmental geology of the Springfield urban area: Association of Missouri Geologists, 20th annual meeting field trip.

25. Orndorff RC, Weary DJ, Lagueux KM (2000): Geographic information systems analysis of geologic controls on the distribution of dolines in the Ozarks of south-central Missouri, USA. - Acta Carsologica 29/2, 161-175, Ljubljana.

26. McCracken M (1971). Structural features of Missouri: Rolla, Missouri Department of Natural Resources, Division of Geology and Water Resources, 99 p.

III. 3D-ELECTRICAL RESISITIVITY TOMOGRAPHY IMAGING OF SUBSURFACE STRUCTURE OF A SINKHOLE IN GREENE COUNTY, MISSOURI

Shishay T. Kidanu*, Evgeniy V. Torgashov, Neil L. Anderson

Department of Geosciences and Geological and Petroleum Engineering, Missouri University of Science and Technology, Rolla, MO 65409, USA.

* Correspondence**:** Email: stkq7f@mst.edu; Tel: +1 573 578 0645

ABSTRACT

A two dimensional (2D) Electrical Resistivity Tomography (ERT) investigation was conducted on a karst sinkhole site in Greene County Missouri (Kidanu et al., 2016) and the results have shown the suitability of the 2D-ERT method to image the subsurface structure of the sinkhole. However, in some situations, 2D-ERT images are less accurate than desired because 2D-ERT processing software cannot compensate for the lateral variations in resistivity that occur outside of the vertical plane of 2D-ERT profile. Three dimensional (3D) changes in resistivity can be mapped using true 3D-ERT acquisition and processing method, but this method tends to be costly and time-consuming. In this study, a convenient alternative called pseudo 3D-ERT method is applied, which is expected to have a higher resolution than the previously done conventional 2D-ERT and significantly less expensive than true 3D-ERT data. Based on borehole control, MASW data and surface observations, it is concluded that the sinkhole is more reliably imaged in the pseudo 3D-ERT dataset than in the 2D-ERT dataset. From the interpretation of the pseudo 3D-ERT it is concluded that the sinkhole developed at the intersection of three vertical joints sets.

Key words: 3D-ERT, MASW, sinkhole.

1. INTRODUCTION

Sinkholes that suddenly collapse can result in loss of human life and property; and ground deformation associated with sinkholes often damage infrastructure such as highways and utilities. For example, the catastrophic sinkhole that developed in Nixa, Missouri, on August 13, 2006, swallowed a car, the garage it was parked in, and part of the adjoining house (Kaufmann, 2008). Furthermore, sinkholes are frequently associated with other hazardous processes and problems (Zhou, 2007; Milanovic, 2000; Kaufmann, 2008). Therefore, investigating the subsurface structure of sinkholes and their development mechanisms enables scientists and engineers to predict subsequent impact and chance of reactivation and provide applicable mitigation measures (Kidanu et al., 2016).

Sinkhole detection using appropriate geophysical techniques is relatively feasible since there is a good contrast between the physical properties of sinkhole fill, which consists of water, air, or soil, and the adjacent strata. Geophysical methods that are commonly used for sinkhole investigation include seismic reflection and refraction (Cook, 1965), gravimetry (Bishop et al., 1997), ground-penetrating radar (Ballard, 1983; Annan et al., 1991), electrical resistivity tomography (Labuda and Baxter, 2001; Roth et al., 2002; Zhou et al., 2002; and Ahmed and Carpenter, 2003), and multichannel analysis of surface waves (Lee et al., 2010; Debeglia et al., 2006). ERT is commonly used in Missouri to investigate the shallow subsurface (depths < 60 m) in karst terrain because the subsurface karst features are generally characterized by highly varying resistivities (Ismail and Anderson, 2012). As stated by Williams (1996) and Cardimona et al. (1998), clays in Missouri are normally characterized by low resistivity (usually less than 50 ohm-m). Residual soils are typically characterized by intermediate resistivity (typically between 25

and 600 ohm-m). Weathered to intact carbonate rock is generally characterized by resistivity (typically more than 125 ohm-m). Air-filled voids are generally characterized by very high resistivity (typically >2000 ohm-m), depending on the conductivity of the encompassing strata and size/shape of the void.

ERT can provide 2D or 3D images of the distribution of the electrical resistivity in the subsurface. The 2D-ERT imaging has been proven to be a suitable technique to map and characterize sinkholes in karst terrain. However, in some situations, 2D-ERT images are less accurate than desired because 2D-ERT processing software cannot compensate for the lateral variations in resistivity that occur outside of the vertical plane of the 2D-ERT profile. Acquisition of real three-dimensional (3D) apparent resistivity data, by placing current electrodes on the nodes of a rectangular grid and measuring all the possible potentials can be used to map 3D changes in resistivity. But this method tends to be costly and time-consuming (Vargemezis et al., 2015; Loke and Barker, 1996). Usually, a cost-effective alternative to image the 3D subsurface apparent resistivity variation is through the application of dense parallel and/or orthogonal surface 2D-ERT lines and process them as though they are true 3D data (Yi et al., 2001; Chambers, et al., 2002). This method has been studied in detail by many authors (Papadopoulos et al., 2006; Gharibi and Bentley, 2005) and their studies have shown that 3D inversion of dense 2D-ERT lines is certainly a surrogate to a real 3D survey and in many times the only fully 3D survey that someone can perform given instrumentation and logistic limitations. Therefore, this 3D resistivity imaging approach is widespread in geophysical practice (Negri et al., 2008; Drahor et al., 2008; Aizebeokhai et al., 2010; Ismail and Anderson, 2012; G. Vargemezis et al., 2015).

2D-ERT investigation was conducted by Kidanu et al., (2016) to image the subsurface structure of a sinkhole in Greene County, Missouri (Figure 1). The result of the investigation has suggested the presence of a linear, vertical, N-S oriented prominently low resistivity anomaly and additional less prominent but seemingly linear, low resistivity anomalies. Furthermore, it is stated that, the prominent N-S oriented anomaly is interpreted as N-S oriented joint set, but the other apparently linear, low resistivity anomalies were not distinct enough to be interpreted as joint sets. The author has recommended further studies to verify these less prominent low resistivity anomalies and better image the 3D-subsurface structure of the sinkhole. Due to the limitations of 2D-ERT profiles, as mentioned earlier, the E-W oriented 2D-ERT profiles in the previous study (Kidanu et al., 2016) might not be capable of detecting linear subsurface features oriented parallel or at an acute angle to the profiles. Therefore, in this research a Pseudo 3D-ERT imaging is generated by processing 2D-ERT data as though they were true 3D data, to characterize the 3D subsurface structure of the sinkhole and get better understanding on its formation and development mechanism.

2. GEOLOGIC AND GEOMORPHOLOGIC SETTING

The study area is located in Southwestern Missouri and its geology consists of mainly the Osagean Series. The area lies on the western side of the Ozark Uplift and the rock layers regionally deep gently towards the west with minor faulting and folding. The bedrock in the study area is the Mississippian age Burlington-Keokuk limestone (Figure 2). This bedrock is characterized by layers of limestone interbedded with thin layers of chert and the presence of chert nodules within the limestone layers. The limestone is a light gray, coarsely crystalline, and nearly pure calcite.

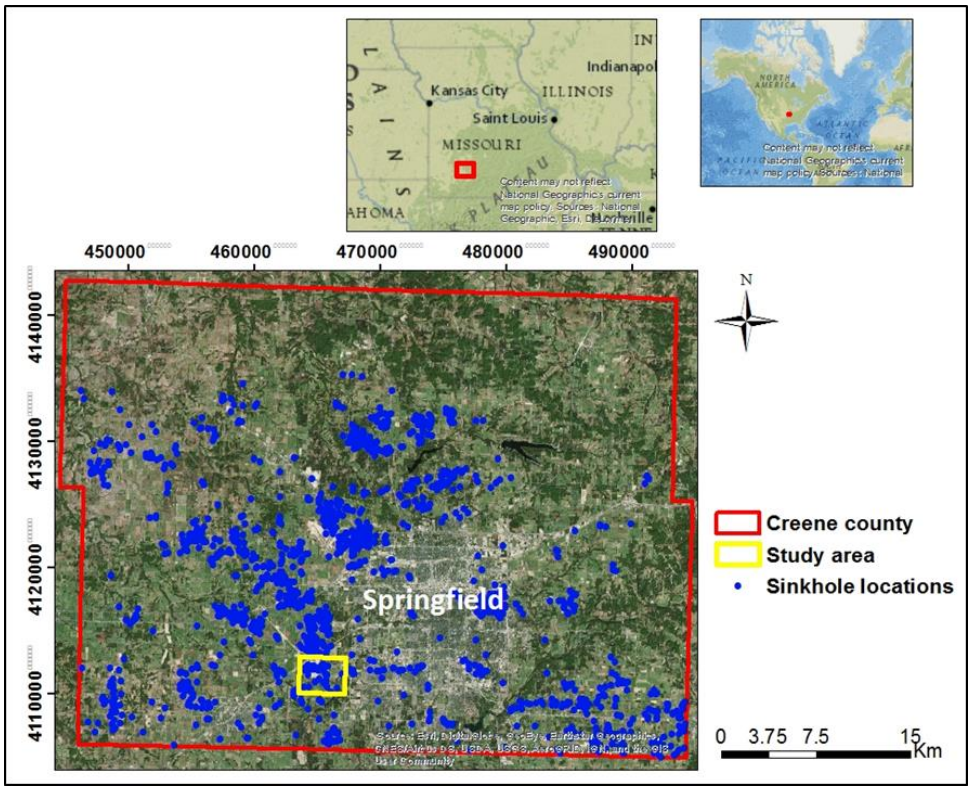

Figure 1. Location map of the study area.

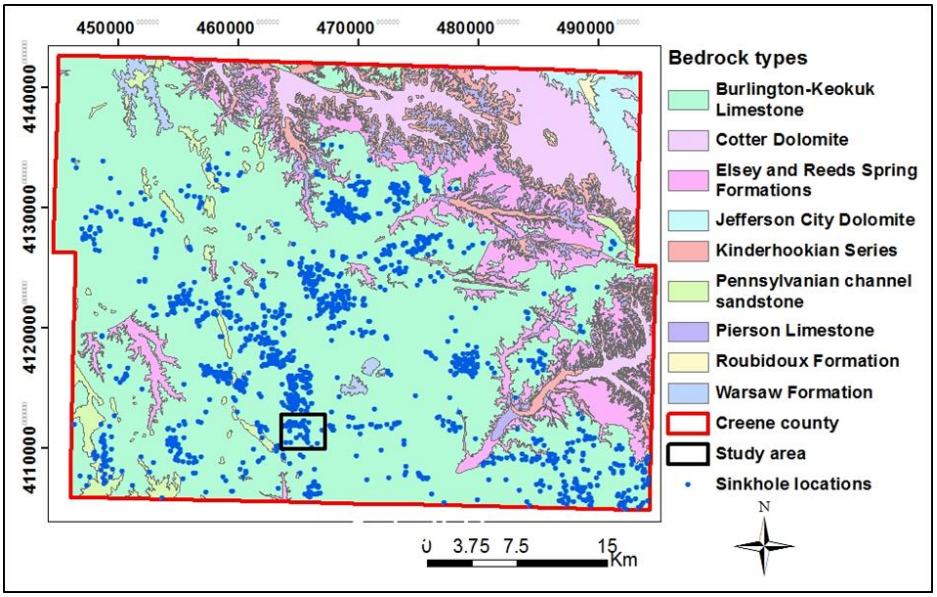

Figure 2. Geological map of Greene County.

Uneven dissolution of the Burlington-Keokuk Formation has resulted in highly irregular bedrock-overburden interface (Fellows, 1970) and is mainly characterized by the formation of prominent knobs (pinnacles) of bedrock bounded by deep troughs (grikes) caused by dissolution in fractures (Figure 3). The thickness of overburden/residuum in Greene County varies from 0 to about 40ft. In many areas stream erosion has removed the overburden and rock is at or very close to the surface, whereas in other areas it reaches to a thickness of about 40 ft.

Figure 3. Carbonate rock outcrops with Cutters and pinnacles (Schultheis, 2013).

According to Randall (2000), the geological structures in southwestern Missouri appear to have controlled the development of karst. As stated by McCracken (1971), the geologic faults in the study area are oriented northwest and northeast. McCracken (1971) has also stated that the bedrock in the study area is characterized by two nearly orthogonal joint sets that exhibit general strike orientations of N 20 º W., and N 60 º E and with vertical dipping.

3. METHODOLOGY

This research used mainly Electrical Resistivity Tomography (ERT). Multichannel Analysis of Surface Waves (MASW) was also used to determine depth to bedrock and aid in the interpretation of the ERT results. Moreover, core logging data from borehole control was also used to verify, constrain and interpret the ERT profiles. Therefore, the interpretations of 2D and 3D ERT data are done based on MASW, borehole control and available pertinent previous data in the study area.

3.1. ELECTRICAL RESISTIVITY TOMOGRAPHY

Electrical resistivity method is used to determine the electrical resistivity of the subsurface by injecting an electrical current (*I*) into the ground through two electrodes (current electrodes) and measuring the electrical potential difference (*V*) at two other electrodes (potential electrodes). The apparent resistivity (ρa) is determined as follows: $\rho a = K \cdot V/I$, where *K* is a geometric factor defined by the electrode array configurations on the surface. The ERT acquisition in this study was performed using an AGI R-8 Supersting multi-channel and multi-electrode resistivity system with 168 electrodes spaced at 1.52m (5ft) intervals and using a dipole-dipole electrode array. Sixteen parallel East-West oriented 2D-ERT profiles of 835ft (254m) long, with 20ft (6.1m) spacing between profiles were acquired over an area in the vicinity of an existing active Sinkhole (Figure 4). These 2D-ERT profiles were used as input for the pseudo 3D-ERT inversion process.

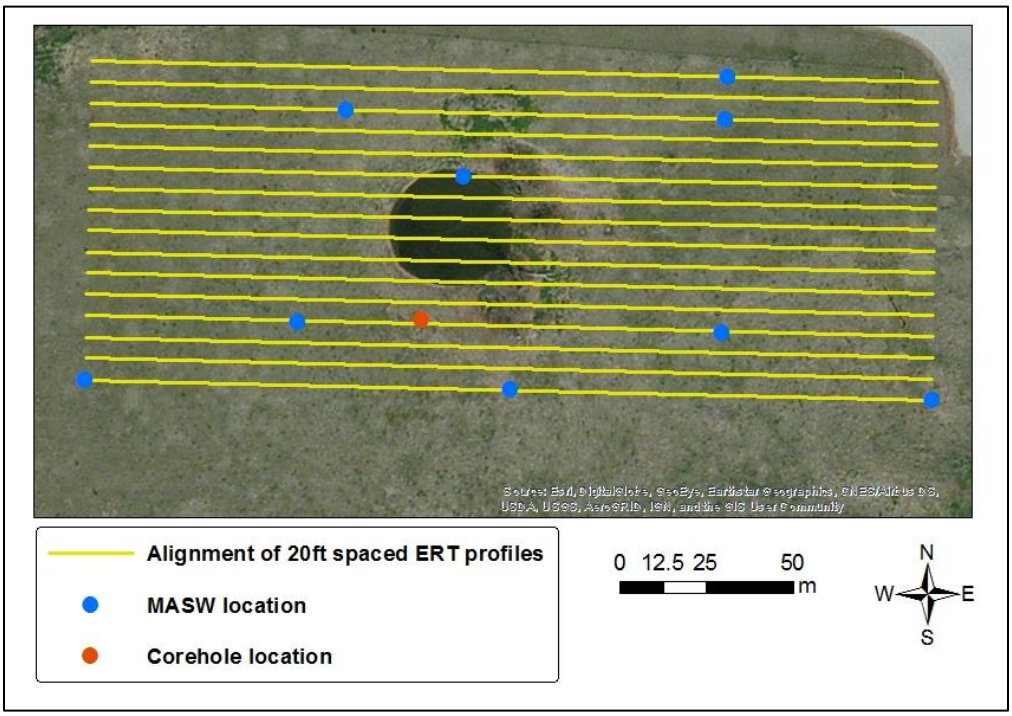

Figure 4. Orientation and location of acquired data.

Both 2-D and 3-D ERT data processing routines were applied to the 2-D ERT data acquired at the sinkhole site with the intent to integrate the 2-D and 3-D images produced from the 2-D resistivity survey to attain better resolution and enhance the interpretation of the resistivity images. Accordingly, the sixteen 2D-ERT data files were later combined into a 3D data file in the RES2DIVN program and inverted using the RES3DINV program (Loke and Barker, 1996b). Sixteen horizontal sections that give planar 2D-ERT image slices with corresponding vertical layer depths were generated from the 3D inversion.

3.2. MULTICHANNEL ANALYSIS OF SURFACE WAVES

In this research MASW was used mainly to determine depth to top of rock and to complement the interpretation of ERT profiles. The locations of the acquired MASW

profiles are given in Figure 4 above. To acquire MASW data the ground is struck with a sledge hammer and the MASW measures the amplitude and arrival time of Raleigh waves. A 24 channel geophone array spaced at typically 2.5 to 5 feet and connected to a seismograph was used to record the seismic data. After acquiring the seismic data, a 1-D shear wave velocity profile of the subsurface was calculated using an inversion process in Surfseis3. In summary, the procedure used for the MASW survey consists of three steps. These are; (i) Data Acquisition---acquiring multichannel field records, (ii) Dispersion Analysis---extracting dispersion curves, and (iii) Inversion---back-calculating shear-wave velocity (Vs) variation with depth (called 1-D Vs profile) that gives theoretical dispersion curves closest to the extracted curves (one 1-D Vs profile from each curve). The NEHRP (National Earthquake Hazard Reduction Program) site classification chart for different geological material, as published in 2000 by the International Building code, provided a basis for the classification of subsurface materials based on their shear wave velocity values. Therefore, the interpretation of the MASW profiles was done based on the NEHRP chart and available borehole control data in the area.

4. RESULTS AND DISCUSSION

4.1. RESISTIVITY AND SHEAR WAVE VELOCITY VALUES

The interpretation of the electrical resisitivity values were made based on the corehole log data, MASW data, and data from previous studies in the area. According to the interpretation; moist soils have resistivity value of less than 125 ohm.m, dry soils greater than 125, moist weathered and/or fractured rock less than 600, fractured rock with moist piped clay fill less than 125, and drier, possibly less weathered/fractured rock greater

than 600 ohm.m. In the MASW data, based on the NEHRP site classification chart and corehole data, a shear wave velocity of less than 1200 feet/sec is typically interpreted as the shear wave velocity of soil.

The resistivity and seismic data interpretation results showed a good fit and consistent correlation with the corehole log data. Specially, the vertical and horizontal 2D-ERT slices from the pseudo 3D-ERT images found to be more consisitent than the actual 2D-ERT data.

4.2. PSEUDO 3D-ERT DEPTH SLICES

A sequence of sixteen horizontal depth slices (layer-1 to layer-16) which extend to a maximum depth of 29.7m were extracted from the 3D-ERT image and are presented in Figure 5a&b. The upper four depth slices (depth range from 0.0m to 2.66m) indicate that the subsurface material in this depth range has mainly low resistivity (<600Ωm) except for some scattered zones of higher resistivity (>600Ωm). The slices from layer-7 (4.67 - 5.9m) to layer-16 (25.4 – 29.7m) show mainly higher resistivity (>600Ωm) zones (bedrock) and some linear low resistivity anomalies which are most likely moist clay-rich vertical joints sets. Depth Slices layer-5 to layer-12 depict two linear prominently low resistivity anomalies trending S 60° W-N 60° E and W-E (Figure 5 a&b, Figure 6). Depth slices layer-12 to layer-16 show similar low resistivity anomalies oriented S 60° W-N 60° E but instead of the W-E anomaly, another S-N oriented anomaly is more prominent in these slices (Figure 5a&b, Figure 7).

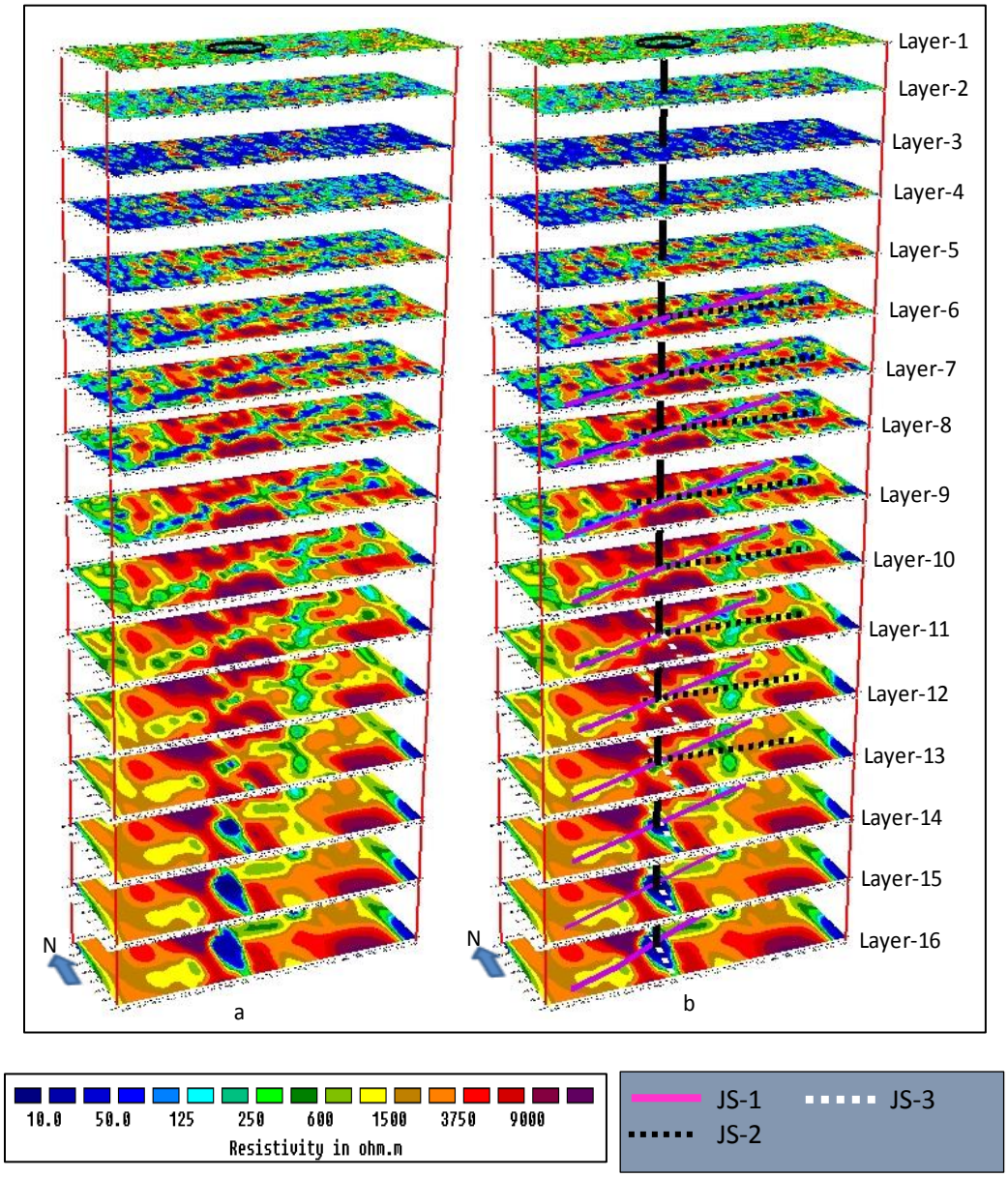

Figure 5. (a) Sixteen ERT-depth slices and location of surface expression of the sinkhole (black circle), (b) ERT-depth slices with the location of the surface expression of the sinkhole and its vertical extrapolation.

It can be seen that the W-E oriented anomaly is not clearly visible on the deepest slices (layer 12 to layer 16), rather the S-N oriented linear anomaly is more visible at these

depths. The most plausible explanation for the fact that the visibility and linearity of the low resistivity anomalies varies vertically (from layer to layer) and laterally (with in a layer) is due to the variation in the amount of moisture and clay content along the joints. The variation in clay and moisture content along joints/fractures is in turn a function of the groundwater flow direction. Therefore, from the 3D-ERT depth slices (Figure 5a), three interpreted joint sets (Figure 5b) have been identified. These three joints sets are labeled as, N-S trending joint set (JS1), E-W trending joint set (JS 2), and S 60° W-N 60° E trending joint set (JS3). Furthermore, an overlay of the location of surface expression of the sinkhole and the 3D-ERTdepth slices (Figure3b) shows that the sinkhole is developed at the intersection of the three joint sets.

The linear, low resistivity anomalies representing the images of joint sets often tend to be wider with depth and have lower resistivity values with an increase in depth. This characteristic of the linear features is visible in both the 2D profiles (Figure 8a) and the 2D-ERT slices extracted from the 3D-ERT image (Figure 8b). This characteristic is attributed most likely to one or combination of the following phenomenon; (1) higher moisture concentrations at depth, (2) the widening of vertical seepage pathways through fractured rocks, and (3) more extensive solution-widening of fractures at depth and increased concentrations of piped clay.

4.3. 3D-MODEL OF SINKHOLE FORMATION AND DEVELOPMENT PROCESS

From preliminary topographic assessment it appears that the vertical, linear low resistivity anomalies interpreted as joint sets have a surface expression characterized by an elongated depression or saddle which are more preferential pathways for surface water.

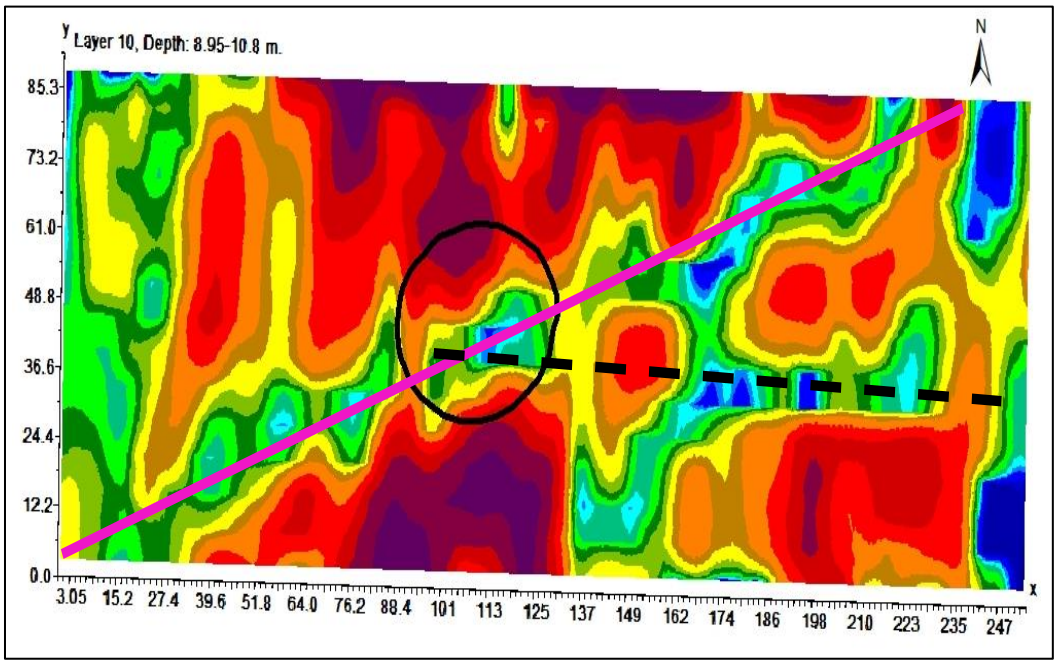

Figure 6. Mainly two linear low resistivity anomaly are visible (SW-NE, and W-E).

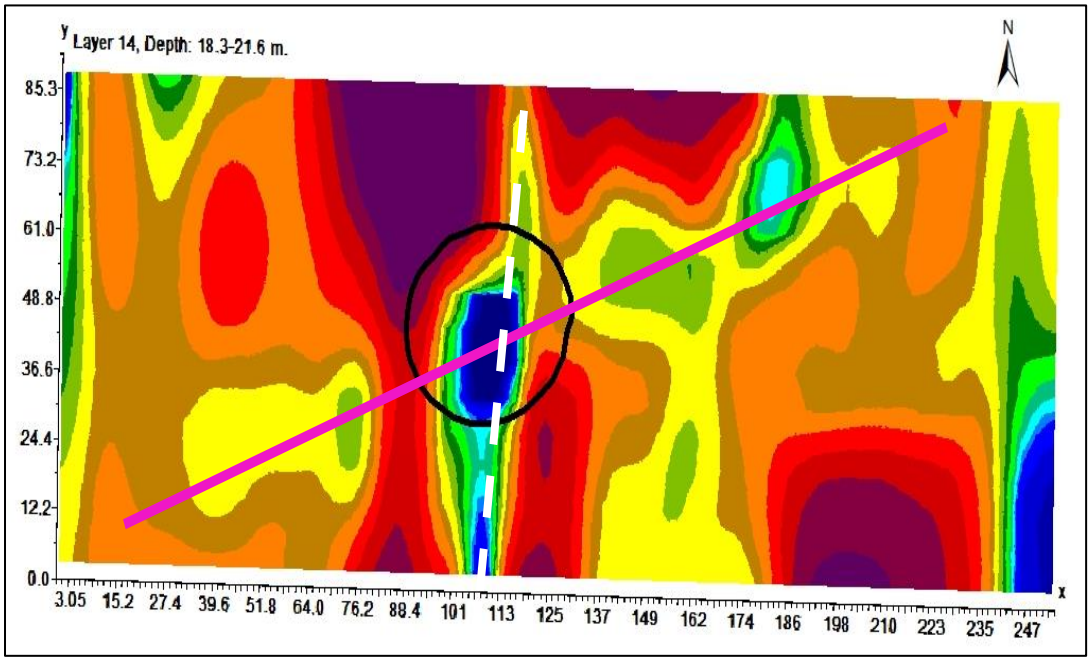

Figure 7. Mainly two linear low resistivity anomaly are visible (SW-NE, and S-N).

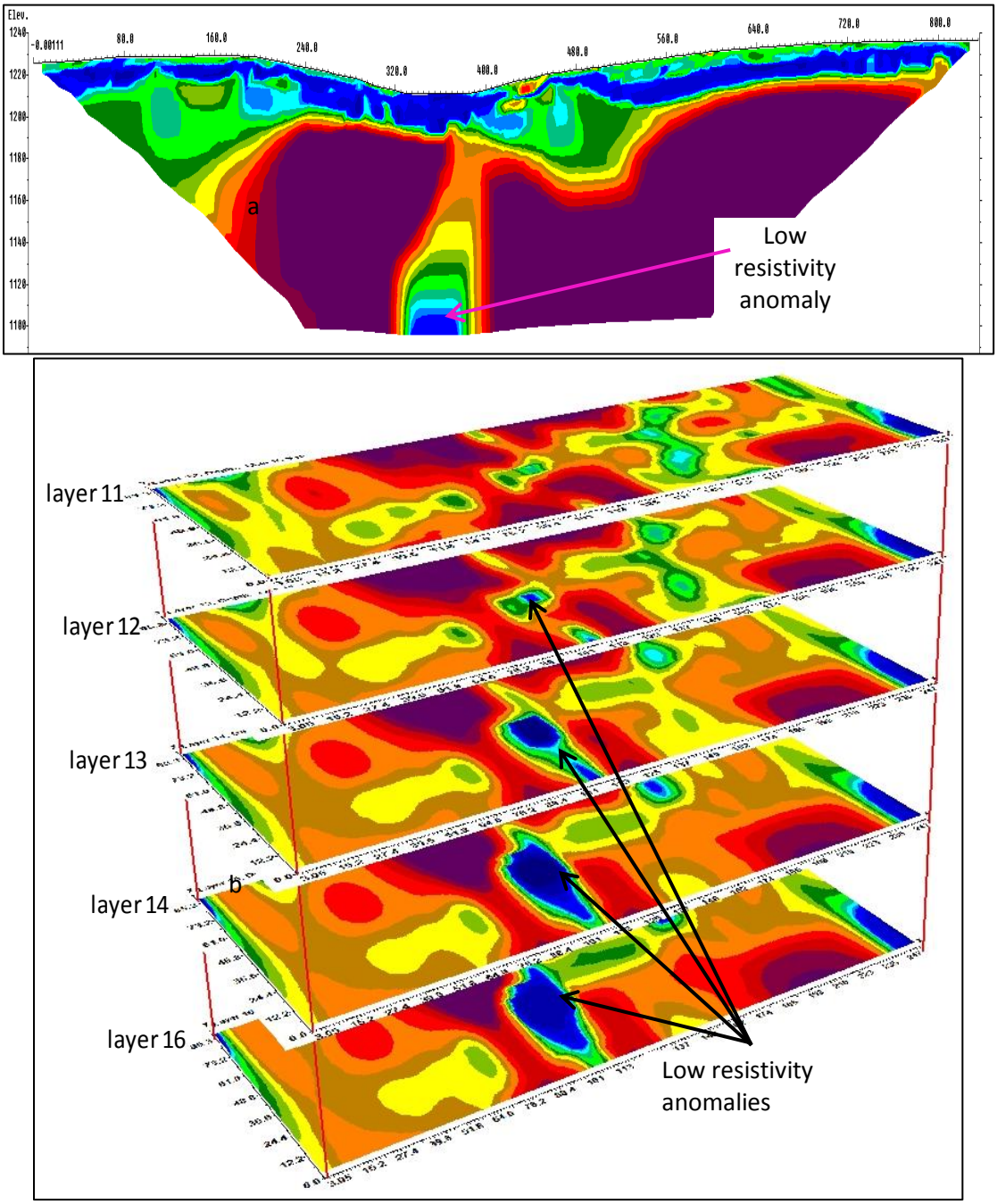

Figure 8. (a) 2D-ERT profile (b) Layers of ERT slices showing the increase in width and the decrease in resistivity value with depth along a vertical low resistivity anomaly.

These implies that the intersection of the three joint sets is relatively the location where more water is first ponded and infiltrated to the subsurface, which is usually the initial stage for the development of subsidence/piping sinkhole. Therefore, from the pseudo 3D-ERT data interpretation and other similar studies in the region, a 3D-model depicting the formation and development process of the sinkhole is developed (Figure 9). The formation and development of the sinkhole involved the following stages of processes: (i) the relatively higher susceptibility for weathering and erosion along joint sets results in the development of elongated depressions and suddle as surface expression of the joint sets which inturn makes the joint sets to be a preferential pathway for surface water flow, (ii) water is ponded at the ground surface above the intersection of the three joint sets and followed by a subsequent infiltration and percolation to the subsurface, (iii) piping of fine grained soils and associated subsidence and minor collapse of residual soils. Previous study by Kidanu et al (2016) has suggested that the sinkhole is not an instantaneous collapse type of sinkhole; rather it appears to have developed gradually and enlarged over time. The soil piping and associated subsidence is a slow and gradual process that continues unless the source of water draining to the sinkhole is retained or blocked. Thus, this kind of sinkhole development can be mitigated using appropriate engineering technologies if the source of piping waters is curtailed.

5. CONCLUSIONS AND RECOMMENDATIONS

2D and Pseudo 3D-ERT methods were used to image the subsurface structure of an active sinkhole in Greene County Missouri. A set of 16 West-East oriented 2D-ERT profiles were acquired as an input for the Pseudo 3D-ERT inversion. The interpretation of

the resistivity properties of the subsurface materials were made based on ground truth corehole data and MASW data.

As compared to the 2D-ERT, the results from the Pseudo 3D-ERT showed a more reliable 3D image of the subsurface structure of the sinkhole and improved the understanding of the sinkhole formation processes. From the Pseudo 3D-ERT interpretation, it is concluded that the sinkhole developed at the intersection of three vertical joints sets (JS-1, JS-2, and JS-3).

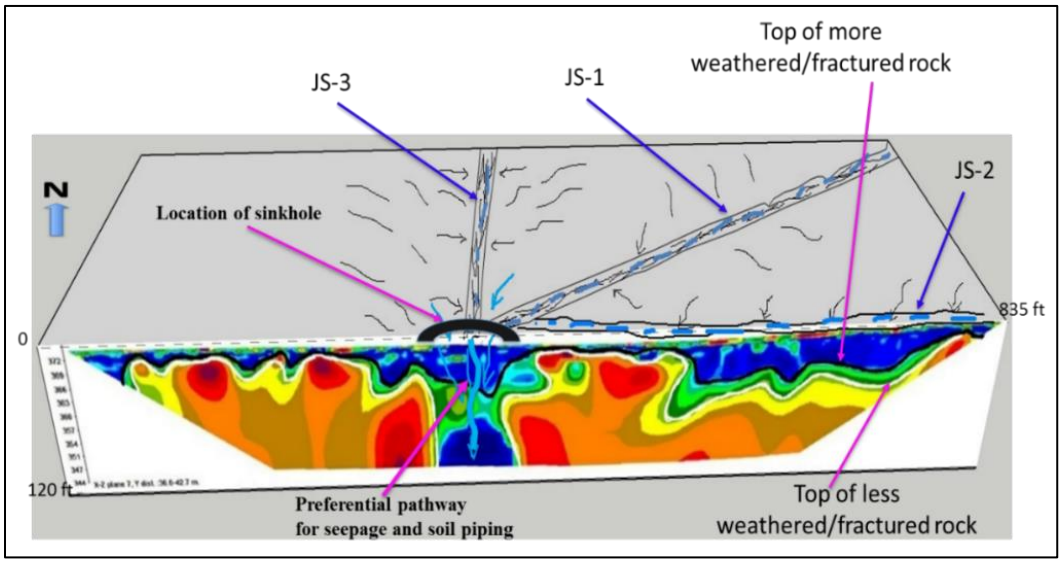

Figure 9. 3D-model, depicting the formation and development process of the sinkhole. JS-1, JS-2 and JS-3 represent joint sets identified based on ERT interpretation.

The interpretation of the ERT images also revealed that there are no major collapse features in the bedrock where the sinkhole developed, except the small soil collapse features deduced from the historical google earth images. Moreover, the interpretation of

the ERT depth slices concerning clay and moisture content implies the presence of soil piping processes. Therefore, this is in agreement with the previous study which stated that the sinkhole is formed due to soil piping which results in gradual ground subsidence and some associated soil collapse. The soil piping and associated subsidence is a slow and gradual process that continues unless the source of water draining to the sinkhole is retained or blocked. Thus, this kind of sinkhole development can be mitigated or halted using appropriate engineering technologies if the source of piping waters is curtailed.

REFERENCES

1. Chalikakis K, Plagnes V, Guerin R, et al. (2011). Contribution of geophysical methods to karst-system exploration: an overview, Hydrogeology Journal, 19: 1169–1180.

2. Festa V, Fiore A, Parise M, et al. (2012). Sinkhole evolution in the Apulian karst of southern Italy; a case study, with some considerations on sinkhole hazards. *Journal of Cave and Karst Studies*, v. 74, p. 137-147.

3. Waltham T, Bell F, Culshaw MG (2005). Sinkholes and Subsidence; Karst and cavernous rocks in engineering and construction. Chichester, UK: Praxis, Springer 382pp.

4. Gutiérrez F (2010). Hazards associated with karst. In Geomorphological Hazards and Disaster Prevention, Alcántara-Ayala I, Goudie A (eds). Cambridge University Press: Cambridge; 161–173.

5. Ahmed I, Neil A (2012). 2-D and 3-D Resistivity Imaging of Karst Sites in Missouri, USA. Environmental & Engineering Geoscience, Vol. XVIII, No. 3, August 2012, pp. 281–293.

6. Carbonel D, Rodríguez V, Gutiérrez F, et al. (2014). Evaluation of trenching, ground penetrating radar (GPR) and electrical resistivity tomography (ERT) for sinkhole characterization, Earth Surf. Process. Landforms, Vol. 39, 214–227.

7. Kaufmann J (2008). A Statistical Approach to Karst Collapse Hazard Analysis in Missouri. Sinkholes and the Engineering and Environmental Impacts of Karst (2008): pp. 257-268.

8. Galve P, Gutiérrez F, Remondo J, et al. (2009). Evaluating and comparing methods of sinkhole susceptibility mapping in the Ebro Valley evaporite karst (NE Spain), *Geomorphology*, v. 111, 160-172.

9. Doctor D, Doctor K (2012). Spatial analysis of geologic and hydrologic features relating to sinkhole occurrence in Jefferson County, West Virginia. Carbonates and Evaporites, 27(2): 143–152.

10. Gutiérrez F, Cooper HA, Johnson KS (2008) Identification, prediction and mitigation of sinkhole hazards in evaporate karst areas. Environ Geol 53:1007–1022.

11. Cook JC (1965) Seismic mapping of underground cavities using reflection amplitudes. Geophysics 30(4):527–538.

12. Bishop I, Styles P, Emsley SJ, et al. (1997). The detection of cavities using the microgravity technique: case histories from mining and karstic environments. Geol Soc Eng Geol Spec Publ 12:153–166.

13. Ballard RF (1983) Cavity detection and delineation research. Report 5, Electromagnetic (radar) techniques applied to cavity detection. Technical Report GL, 83–1, pp 90.

14. Annan AP, Cosway SW, Redman JD (1991) Water table detection with ground-penetrating radar. In: Soc. Explor. Geophys (Annual International Meeting Program with Abstracts), pp 494–497.

15. Labuda TZ, Baxter AC (2001), Mapping karst conditions using 2D and 3D resistivity imaging methods, paper presented at the Symposium on the Application of Geophysics to Engineering and Environmental Problems (SAGEEP), Environ. and Eng. Geophys. Soc., Denver, Colorado.

16. Roth MJS, Mackey JR, Mackey C, et al. (2002). A case study of the reliability of multi-electrode earth resistivity testing for geotechnical investigations in karst terrains, Eng. Geol., 65, 225–232.

17. Zhou W, Beck BF, Adams AL (2002). Effective electrode array in mapping karst hazards in electrical resistivity tomography. Environ. Geol. 42:922–928.

18. Ahmed S, Carpenter PJ (2003). Geophysical response of filled sinkholes, soil pipes and associated bedrock fractures in thinly mantled karst, east-central Illinois. Environmental Geology, 44:705–716.

19. Lee R, Callahan P, Shelly B, et al. (2010). MASW Survey Identifies Causes of Sink Activity Along I-476 (Blue Route), Montgomery County, Pennsylvania. In: GeoFlorida 2010 Conference; Feb. 20-24.

20. Debeglia N, Bitri A, Thierry P (2006). Karst investigations using microgravity and MASW; application to Orleans, France. Near Surface Geophysics 4: 215–225.

21. Odum JK, Williams RA, Stephenson WJ, et al. (2007). Near-surface shear wave velocity versus depth profiles, Vs 30, and NEHRP classifications for 27 sites in Puerto Rico:USGS Open-File Report 2007-1174.

22. Waltham AC, Fookes PG (2005). Engineering classification of karst ground conditions. Speleogenesis and Evolution of Karst Aquifers, the Virtual Scientific Journal ISSN 1814-294X.

23. Vandike JE (1993) Groundwater level data for Missouri: Water year 1991-1992. Missouri Department of Natural Resources. Division of Geology and Land Survey. Water Resource Report No.42. Rolla, Missouri.

24. Fellow LD (1970). Geology of Galloway Quadrangle Greene County Missouri, Missouri Geological Survey and Water Resources, pp 3-14.

25. Hayes WC, Thomson KC (1973). Engineering and environmental geology of the Springfield urban area: Association of Missouri Geologists, 20th annual meeting field trip.

26. Orndorff RC, Weary DJ, Lagueux KM (2000): Geographic information systems analysis of geologic controls on the distribution of dolines in the Ozarks of south-central Missouri, USA. - Acta Carsologica 29/2, 161-175, Ljubljana.

27. McCracken M (1971). Structural features of Missouri: Rolla, Missouri Department of Natural Resources, Division of Geology and Water Resources, 99 p.

SECTION

2. CONCLUSIONS

The Burlington-Keokuk Limestone bedrock underlies more than 70% of Greene County and 98 % of the identified sinkholes in the county (Missouri Geological Survey-GeoSTRAT, 2016) formed in this unit. Analysis of the sinkholes' spatial distribution and patterns suggest that the sinkholes are not randomly distributed, but are spatially clustered. GIS-based multivariate regression methods (OLS and GWR) were applied to evaluate the spatial relationships between potential sinkhole influencing factors (explanatory variables) and sinkhole density (dependent variable), with the aim of evaluating the significant controlling factors. The OLS analysis revealed that seven of the twelve possible influencing factors considered in the analysis likely play important roles in triggering the formation of sinkholes. These factors are overburden thickness, slope of ground surface, depth to groundwater, distance to the nearest drainage line, distance to the nearest road, distance to the nearest geological structure, and distance to the nearest spring. GWR improved the model and explained 86% (better than OLS=57%) of the sinkhole density variability. The GWR model coefficient values for each explanatory variable provide visual insight into the influence of these variables on localized sinkhole density and patterns, and the values can be used to provide an objective means of parameter weighting in models of sinkhole susceptibility or hazard mapping/zoning. The OLS and GWR models were able to explain only 57% and 86% of the processes responsible for the formation of mapped sinkholes, respectively. Therefore further research incorporating more data with better resolution is recommended to improve the model.

In the site-specific geophysical investigations, two dimensional (2D) and pseudo three dimensional (3D) - ERT (electrical resistivity tomography), MASW (multichannel analysis of surface waves), and borehole data were used to characterize the subsurface morphology of the karstified soil-bedrock interface in five selected sinkholes. The detailed investigation of one of the selected sinkholes is presented in the second and third paper. From the interpretation of the 2D and pseudo 3D-ERT profiles, it was determined that four of the five sinkholes occurred at the intersections of regional systematic joint sets. The joint sets are characterized by a linear, visually prominent zones of low resistivity. The relatively low resistivity values are attributed to vertical seepage and the associated piping of fine-grained soils through preexisting fractures (often widened by solutioning). The soil piping and associated subsidence is a slow and gradual process that continues unless the source of water draining to the sinkhole is retained or blocked. Thus, this kind of sinkhole development can be mitigated or halted using appropriate engineering technologies if the source of piping waters is curtailed.

VITA

Shishay Tadios Kidanu was born in Shire, Tigray, Ethiopia. He received his Bachelor of Science degree in applied geology in 2004 from Mekelle University, Ethiopia and Master of Science degree in Earth Sciences in 2008 from Graz University of Technology, Graz, Austria. Shishay was employed as a faculty at department of Earth sciences at Mekelle University, Ethiopia from 2008 to 2013.

In August 2013, Shishay started his Ph.D. study at Missouri University of Science and Technology. During his Ph.D. study, Shishay worked as a graduate Research and Teaching Assistant in the Geological Engineering program. He was directly involved in numerous Geophysical investigation projects. Shishay has presented his research work in a number of conferences and has also published articles in peer reviewed journals.

He obtained his Ph.D. in Geological Engineering from Missouri University of Science and Technology in May 2018.